CARPE DIEM
CENTRE FOR WATER RESOURCES RESEARCH
DELIVERABLE 9.5(NUID-CWRR)
PRECIPITATION DATA ANALYSIS AND ERRORS
DRAFT

by
Micheal Bruen & Benoit Parmentier

December 2004
Department of Civil Engineering
University College Dublin

Table of Contents

List of Tables

List of Figures

Chapter 1

Criteria for Radar data assessment for use in flood monitoring and forecasting

1.1 Introduction

The radar rainfall product (refer to Chapter **??** provided by Met Eireann is considered as the basis for the following analyses. No specific corrections to the reflectivity data are carried out. The surface rainfall intensity data are used for comparisons with raingauges, for the calculations of adjustment factors and as input to hydrological models for flood estimation.

Adjustment factors are defined below. They are used to correct raw the surface rainfall intensity radar data. Performance criteria are also defined to assess the quality of the rainfall and flow rate estimates obtained using the different sources of information.

1.2 Adjustment factors

An adjustment factor is a constant by which a raw radar estimate of precipitation can be multiplied to obtain a corrected precipitation estimate. We distinguish between uniform and spatial adjustment factors. Please refer to Chapter **??** for an introduction to radar estimates correction techniques.

Uniform adjustment factors are the simplest adjustment technique. The mean radar bias is computed using all the raingauges and corresponding radar pixels data available in the

catchment considered. The radar estimates can then be multiplied by the adjustment factor (also called correction factor). Wilson (1970) applied the case to a 3500 km^2 catchment and found a reduction in the mean error from 51% down to 35%.

When several raingauges data are available, an adjustment factor can be computed for each raingauge. The corrections of radar data are then carried out using the adjustment factor of the single closest raingauge to the radar estimate location. Errors have been shown to be smaller than by considering an average adjustment factor for the ensemble of raingauges available in the same area.

Six different methods of calculation of the adjustment factors are tested here. They are all based on the ratios of raingauge to radar measurements of precipitation G/R. In the following, $G_{i,T}$ denotes the precipitation accumulation during one time step at raingauge i at time T, and $R_{i,T}$ denotes the precipitation accumulation during one time step in the radar pixel corresponding to the location of raingauge i at time T, estimated from raw radar rainfall intensity data. n denotes the total number of time steps used in the analysis. N denotes the number of raingauges. Note that the denomination of the adjustment factors is subjective.

1.2.1 Uniform adjustment factor Type 1: A_{U1}

The spatial adjustment factor A_{U1} is defined as follows:

$$A_{U1} = \frac{1}{n} \sum_{T=1}^{T=n} \left[\frac{\sum_{i=1}^{i=N} G_{i,T}}{\sum_{i=1}^{i=N} R_{i,T}} \right] \tag{1.1}$$

where the summation is taken only over the time steps for which with $G_{i,T} > Min$ and $R_{i,T} > Min$ where Min is a minimum strictly positive, selected to avoid division by zero and the consideration of extreme fractions, when $R_{i,T} \ll G_{i,T}$. A minimum of $0.2mm$ for a 1 hour accumulation is selected (Wood et al., 2000).

1.2.2 Uniform adjustment factor Type 2: A_{U2}

The spatial adjustment factor A_{U2} is defined as follows:

$$A_{U2} = \frac{1}{n} \sum_{T=1}^{T=n} \left[\frac{1}{N} \sum_{i=1}^{i=N} \frac{G_{i,T}}{R_{i,T}} \right] \tag{1.2}$$

with $G_{i,T} > Min$ and $R_{i,T} > Min$ where Min is a minimum strictly positive, selected to avoid division by zero and the consideration of extreme fractions, when $R_{i,T} \ll G_{i,T}$. A minimum of $0.2mm$ for a 1 hour accumulation is selected (Wood et al., 2000).

1.2.3 Uniform adjustment factor Type 3: A_{U3}

The spatial adjustment factor A_{U3} is defined as follows:

$$A_{U3} = \frac{\sum_{T=1}^{T=n} \sum_{i=1}^{i=N} G_{i,T}}{\sum_{T=1}^{T=n} \sum_{i=1}^{i=N} R_{i,T}} \tag{1.3}$$

1.2.4 Spatial adjustment factor Type 1: A_{S1}

The spatial adjustment factor A_{S1} is defined as follows:

$$A_{S1} = \frac{1}{n} \sum_{T=1}^{T=n} \frac{G_{i,T}}{R_{i,T}} \tag{1.4}$$

with $G_{i,T} > Min$ and $R_{i,T} > Min$ where Min is a minimum strictly positive, selected to avoid division by zero and the consideration of extreme fractions, when $R_{i,T} \ll G_{i,T}$. A minimum of $0.2mm$ for a 1 hour accumulation is selected (Wood et al., 2000).

1.2.5 Spatial adjustment factor Type 2: A_{S2}

The spatial adjustment factor A_{S2} is defined as follows:

$$A_{S2} = \frac{\sum_{T=1}^{T=n} G_{i,T}}{\sum_{T=1}^{T=n} R_{i,T}} \tag{1.5}$$

1.2.6 Spatial adjustment factor Type 3: A_{S3}

The spatial adjustment factor A_{S3} is defined as follows:

$$A_{S3} = \frac{\sum_{T=1}^{T=n} R_{i,T} G_{i,T}}{\sum_{T=1}^{T=n} R_{i,T}^2} \tag{1.6}$$

This is a new adjustment factor that minimises the sum of squares of the residuals between the raingauge and the radar series, thus optimising the correction for high values of precipitation. However, this adjustment factor does not verify the conservation of rainfall volumes, and should be used with caution.

1.3 Performance criteria for rainfall estimation

The statistics computed for comparing radar and raingauge rainfall estimates are listed below. For a visual comparison of rainfall intensity and accumulation estimates, charts can also produced using the GIS package (see Chapter **??**).

1.3.1 Descriptive statistics

Simple statistics for each type of rainfall estimates can be computed. They include the sum, average, standard deviation, minimum and maximum values, number of values above some threshold.

1.3.2 Correlation

Correlation coefficients can be computed to investigate the relationship between two data time-series. A high correlation coefficient, close to 1, is indicative of a strong correlation between the two rainfall estimates series.

1.3.3 Coincidence of a measurement

The number of following cases may be counted:

1. Both radar and raingauge estimates are stricly positive,
2. Radar value is zero, raingauge value is stricly positive,
3. Radar value is strictly positive, raingauge value is zero,
4. Both radar and raingauge estimates are zero.

Those statistics indicate in how many cases the radar and the raingauge detect precipitation at the same time, and in how many cases one instrument detects precipitation while the other one does not detect precipitation.

1.3.4 Residuals, Mean absolute error and Nash coefficient

$G_{i,T}$ denotes the raingauge one time-step accumulation at location i and time T, and $Re_{i,T}$ denotes the one time-step estimated accumulation in the radar pixel corresponding to the

location of raingauge i at time T (this is not necessarily the raw radar value $R_{i,T}$, and may involve the correction of the raw estimate). n denotes the total number of time steps used in the analysis.

The means of residuals, noted MRs is the mean of the differences between two data series:

$$MRs = \frac{1}{n} \sum_{i=1}^{n} \left(Re_{i,T} - G_{i,T} \right) \tag{1.7}$$

It gives us information on the radar estimates bias.

The maximum and minimum values of the residuals can be given to evaluate the extreme errors.

The mean square error, noted MSE, is given by:

$$MSE = \frac{1}{n} \sum_{i=1}^{n} \left(Re_{i,T} - G_{i,T} \right)^2 \tag{1.8}$$

The MAE criterion is defined as:

$$MAE = \frac{1}{n} \sum_{i=1}^{n} \left| Re_{i,T} - G_{i,T} \right| \tag{1.9}$$

The Nash criterion is defined below in **??** for flow rates data. Q_o becomes G and Q_c becomes Re.

Chapter 2

Analysis of radar rainfall estimates

2.1 Introduction

The high resolution, high quality hydrological database created provides the opportunity to perform an extensive analysis of the value of radar data. Their usefulness in terms of direct precipitation measurements and in terms of source of inputs for hydrological models is investigated. The evaluation looks at: (1) the quality of radar estimates of precipitation in this Chapter and (2) its usefulness in conjunction with hydrological models for simulating and forecasting floods in the next Chapter.

Radar Surface Intensity Rainfall data are converted into rainfall accumulation data and then those are used to compute the different adjustment factors. Different types of precipitation estimates are defined (e.g. raw radar or adjusted radar data). The first comparison is of raw and adjusted radar data with raingauge data.

2.2 Radar adjustment factors

To compute the adjustment factors, the radar and raingauge data at the same location for the entire calibration year 2002/2003 were considered. Adjustment factors were computed for different time steps: 15 minutes, 1 hour and 1 day, as shown on Tables 2.2, 2.3 and 2.4. For comparison only, the corresponding adjustment factors were also computed for the validation year 2003/2004 for the 1 hour time step. Table 2.1 contains the yearly accumulations in mm for the raingauge and their corresponding radar pixels and it is clear that the radar under-estimates the true rain.

In the following, H0203 and H0304 denote hydrological year 2002/2003 and 2003/2004

respectively. 01,02,03,04 are the ID for raingauges at Djouce, Powerscourt, Stone and Bray respectively. The number in brackets following the adjustment factor name in some cases is the minimum rainfall accumulation value selected for its computation.

Estimate	H0203				H0304			
	01	02	03	04	01	02	03	04
Raingauge	1580.3	1350.4	1422.6	1249.2	1272.1	1032.8	1190.0	828.6
Radar	518.9	518.0	439.5	555.9	382.0	372.8	363.9	341.9

Table 2.1: Yearly precipitation accumulations in mm.

Adjustment factor	H0203			
	01	02	03	04
$A_{S1}(0.0)$	6.44	4.68	6.55	5.09
$A_{S1}(0.05)$	3.27	2.72	3.33	2.69
$A_{S1}(0.2)$	2.44	2.13	2.67	2.06
A_{S2}	3.05	2.61	3.24	2.25
A_{S3}	1.64	1.48	1.97	1.19
	Uniform			
$A_{U1}(0.0)$	7.84			
$A_{U1}(0.05)$	3.99			
$A_{U1}(0.2)$	2.77			
$A_{U2}(0.0)$	6.47			
$A_{U2}(0.05)$	2.99			
$A_{U2}(0.2)$	2.25			
A_{U3}	2.76			

Table 2.2: Adjustment factors for 15 minutes time step.

Year 2002/2003 is noticeably wetter than year 2003/2004, as indicated by the yearly amounts for all the rainfall estimates on Table 2.1. This is due to extreme storms at the end of 2002, between November and December.

Although the Dublin weather radar was not functioning during a period of 3 weeks (August-early September) in 2003 and 2004, this has practically no effect on the values of the adjustment factors. The reason being that the period covering August and early September 2003 was exceptionally dry and that the corresponding period in 2004, although

Adjustment factor	H0203				H0304			
	01	02	03	04	01	02	03	04
$A_{S1}(0.0)$	6.58	4.71	7.07	5.46	6.16	4.92	5.24	4.62
$A_{S1}(0.2)$	3.01	2.60	3.03	2.44	2.79	2.52	2.70	2.48
A_{S2}	3.05	2.61	3.24	2.25	3.32	2.77	3.26	2.42
A_{S3}	1.92	1.71	2.21	1.41	2.01	1.81	2.15	1.52
	Uniform				Uniform			
$A_{U1}(0.0)$	8.18				7.02			
$A_{U1}(0.2)$	3.38				3.23			
$A_{U1}(0.4)$	2.97				2.81			
$A_{U1}(0.8)$	2.66				2.53			
$A_{U2}(0.0)$	6.65				6.07			
$A_{U2}(0.2)$	2.78				2.68			
A_{U3}	2.76				2.96			

Table 2.3: Adjustment factors for 1 hour time step.

wetter, contributes only a small fraction of the annual rainfall.

The values obtained for year H0203 are very similar to the ones obtained for year H0304 for the 1 hour time step. It is therefore reasonable to assume adjustment factors constant in time, and to apply the adjustment factors determined from the calibration only to the radar data for the two years.

Adjustment factor A_{S3} is noticeably smaller than any other adjustment factor. This adjustment factor is new and minimises the errors between radar and raingauge estimates. However, it does not account for volumetric correction, as the yearly corrected radar data accumulations do not match the yearly raingauge accumulations.

The minimum value selected, when required, influences the final estimate of the adjustment factor. A minimum of 0 mm is not acceptable. The value of 0.2 mm gives values that correspond to the other adjustment factors values.

Overall, most adjustment factors value are found to lie in the range [2.5-3.5] and those values are expected from the review of the literature on adjustment factors.

Adjustment factor	H0203			
	01	02	03	04
$A_{S1}(0.0)$	5.47	5.39	6.06	5.81
$A_{S1}(0.2)$	3.87	2.88	3.85	2.68
$A_{S1}(5.0)$	2.76	2.32	2.74	2.15
A_{S2}	3.05	2.61	3.24	2.25
A_{S3}	2.66	2.43	2.86	2.04
	Uniform			
$A_{U1}(0.0)$	5.75			
$A_{U1}(0.2)$	3.65			
$A_{U1}(20.0)$	2.44			
$A_{U2}(0.0)$	6.19			
$A_{U2}(0.2)$	3.37			
$A_{U2}(5.0)$	2.49			
A_{U3}	2.76			

Table 2.4: Adjustment factors for 1 day time step.

2.3 Types of precipitation estimates

Different types of precipitation estimates were derived for the analysis. They include raingauge, raw radar and adjusted radar data. They are defined in Table 2.5 below. The data from those different types of precipitation are used subsequently for the analysis of the precipitation and as inputs into hydrological models for the analysis of flow rate estimates.

Adjustment factors A_{S2}, A_{S3} and A_{U3} were used to correct radar rainfall estimates. The other adjustment factors being very similar, no computation was required using them. Adjustment factors computed for a given time step were used to correct the precipitation accumulations for the same time step. In the following, "radar" means radar estimate at raingauge location, "all radar" means all the radar estimates over the specified area. Thiessen means the rainfall estimates are given for each Thiessen polygon over the catchment for use as input into a distributed or semi-distributed hydrological model. Otherwise, they are of uniform type and may be used as input into any type of hydrological model.

Type	Description	Spatial type
T1	raingauges	Thiessen
T2	radar	Thiessen
T31	radar adjusted A_{S2}	Thiessen
T32	radar adjusted A_{S3}	Thiessen
T4	average raingauges	uniform
T5	average radar	uniform
T61	average radar adjusted A_{S2}	uniform
T62	average radar adjusted A_{S3}	uniform
T7	average all radar over catchment area	uniform
T81	average all radar over catchment area adjusted A_{S2}	uniform
T82	average all radar over catchment area adjusted A_{S3}	uniform
T83	average all radar over catchment area A_{U3}	uniform
T9	average all radar over respective Thiessen area	Thiessen
T101	average all radar over respective Thiessen area adjusted A_{S2}	Thiessen
T102	average all radar over respective Thiessen area adjusted A_{S3}	Thiessen

Table 2.5: Types of precipitation estimates.

2.4 Comparison of different types of precipitation estimates

The Dublin Airport weather radar was down due to maintenance operations during the two following periods: from 12 August 2003 to 2 September 2003 (in H0203) and from 14 August 2004 to 7 September 2004 (in H0304). The data for those periods are excluded for the analysis.

Figures 2.1, 2.2 and 2.3 show charts created with the GIS package to compare rainfall estimates. The radar is correlated to the raingauge, but it under estimates the precipitation noticeably.

2.4.1 15 minutes rainfall accumulations

The following precipitation estimates types are used for the 15 minutes data analysis: T1, T2, T31 and T32. The raw raingauge data (Type 1) were used as the reference to which the other data types are compared. Data of types T9, T101 and T102 were not used for the 15 minutes analysis because of computation requirements. The computations are carried out for each raingauge case.

Table 2.6 and 2.7 shows the descriptive statistics for the 4 raingauge locations for the

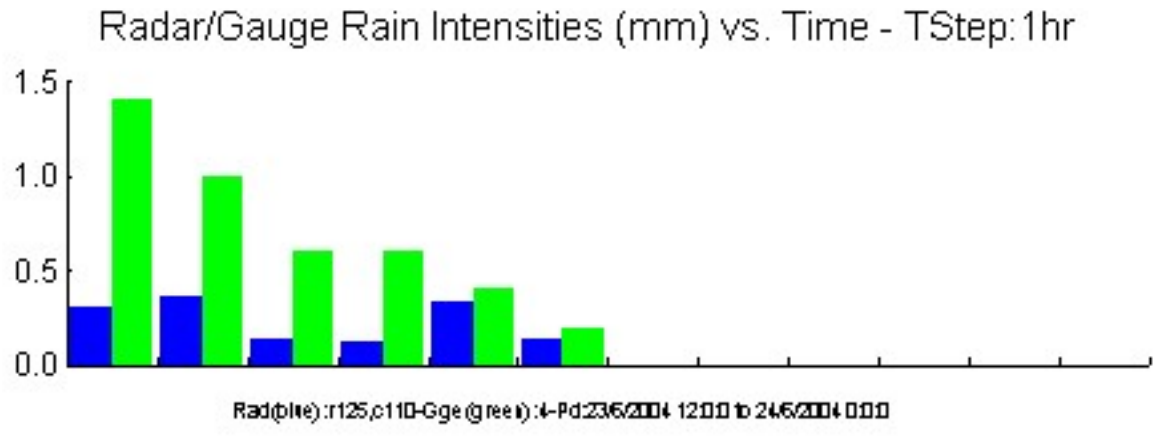

Figure 2.1: Rainfall measurements at Bray for 1 hour accumulations

calibration year (H0203) and the validation year (H0304). The comparative statistics are shown on Table 2.8 and Table 2.9 for H0203 and H0304.

Year H0203 was a wet year if compared to the long term average, whereas year H0304 was rather dry, as it is shown by the sums. From the highest raingauge total to the lowest total, the locations may be ranked: Djouce, Stone, Powerscourt and Bray. This is not true for the radar estimates. Raw radar data hardly ever exceed the threshold of 2 mm. Rainfall T31 shows the closest statistics to the raingauge rainfall T1. Rainfall T32 does not match T1 in terms of volume, only reaching about half the annual volume.

Rainfall T2 and T32 show a negative bias whereas rainfall T31 shows no bias. Rainfall T32 optimises the Nash and the MSE in all cases. The correlation coefficients vary between 0.64 and 0.71 over the two years and are relatively similar in magnitude. There are more cases when the radar detects precipitation and the raingauge does not than the reverse, except for Powerscourt in the calibration year. A possible reason is the time of fall of the hydrometeors between the 1000 m altitude above ground and the ground level.

The validation year shows overall better results than the calibration year. This is possibly due to the fact that the second year was much drier than the first year. The best data are the T32 in terms of MSE and Nash, and the T31 in terms of Bias (MRs).

2.4.2 1 hour rainfall accumulations

A correlation analysis of the hourly rainfall accumulations for the four raingauges was conducted. In the calibration year, the correlation coefficient varies between 0.84 and 0.90.

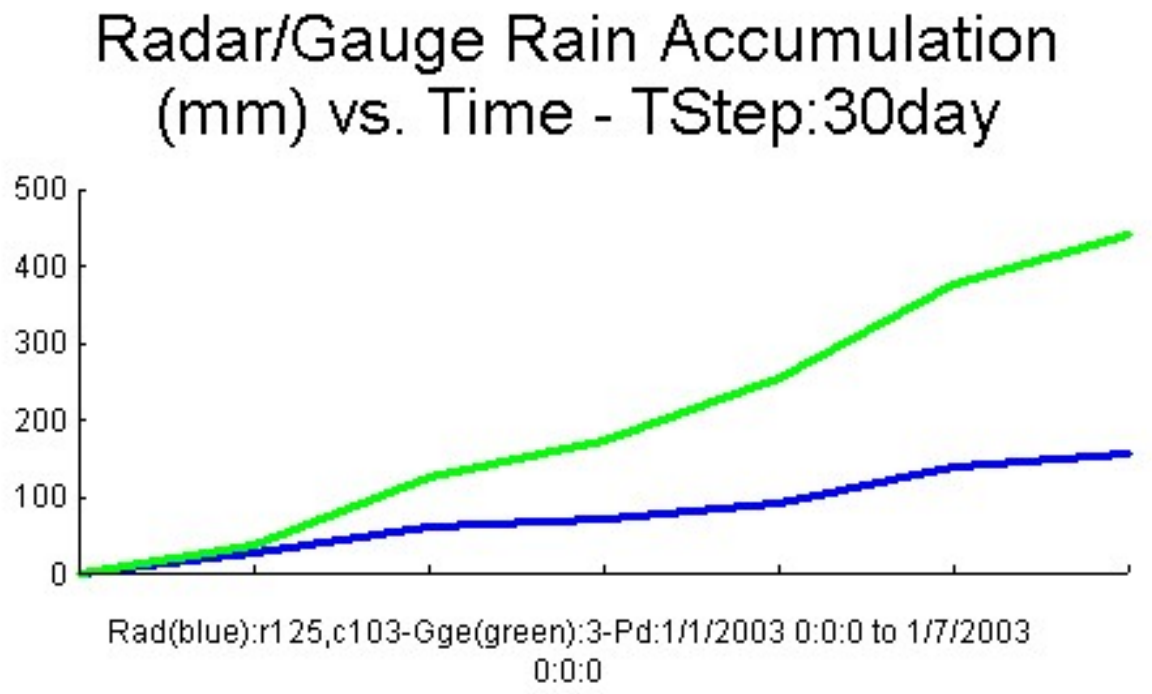

Figure 2.2: Rainfall cumulative chart at Stone

In the validation year, the same parameter varies between 0.76 and 0.87. It is expected that the raingauges accumulations are highly correlated, due to the density of the raingauge network.

The following precipitation estimates types are used for the 1 hour data analysis: T1, T2, T31, T32, T9, T101 and T102. The raw raingauge data (Type 1) were used as the reference to which the other data types are compared. The computations are carried out for each raingauge case.

Table 2.10 and 2.11 shows the descriptive statistics for the 4 raingauge locations for H0203 and H0304. The comparative statistics are shown on Table 2.12 and Table 2.13 for H0203 and H0304.

Raw data T1 and T2 confirm that the year H0304 was much drier than year H0203. Raw radar estimates hardly exceed 5 mm and never exceed 10 mm, whereas the raingauges exceed the latter threshold a few times.

Radar data always show negative bias, except when corrected with A_{S2} adjustment factor (T31 and T101). A_{S3}, used with T32 and T102, optimises the MSEa and Nash. The correlation coefficients are higher than for the 15 minutes accumulations (between 0.72 and 0.81).

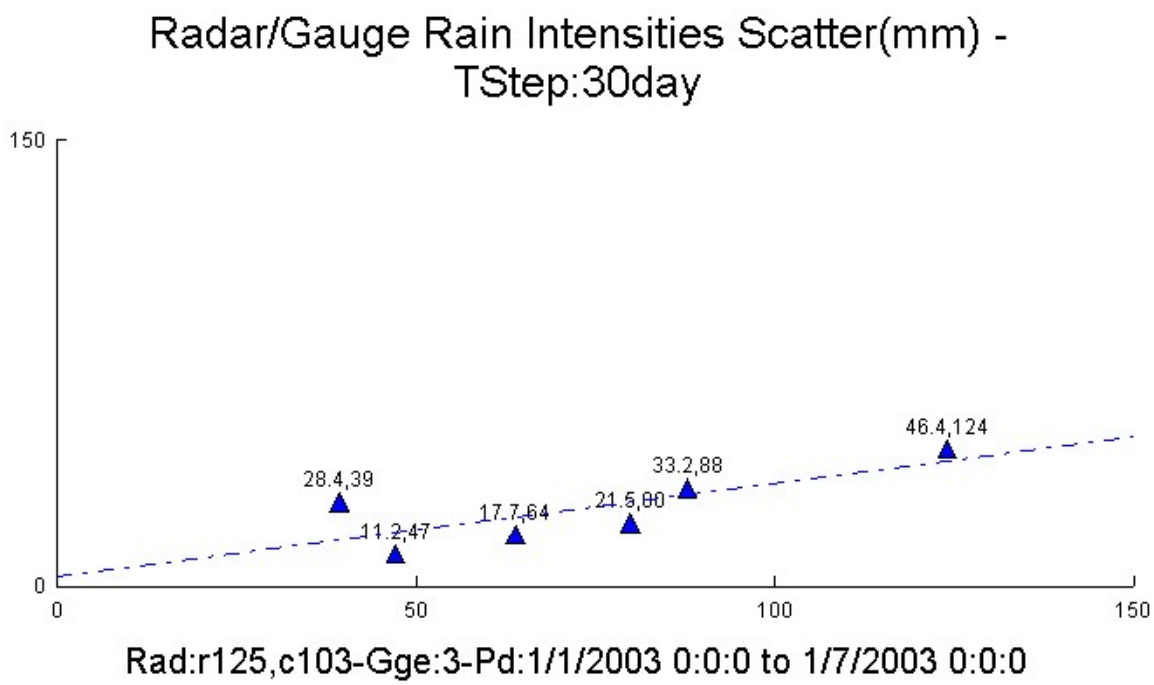

Figure 2.3: Rainfall scatter plot for Stone

In contrast to the results for the 15 minutes accumulations, the occurrence of "radar detects/raingauge does not detect" is less than the opposite case for most locations, except for T9, T101 and T102. The accumulations over longer periods reduces the effect of suspected time shift due to the time of fall of the hydrometeors.

The results in terms of MSE and bias are better for the validation year than the calibration year for the same reason. The best data are the T32 and T102 in terms of MSE and Nash, and the T31 and T101 in terms of Bias (MRs).

2.4.3 1 day rainfall accumulations

The same types of precipitation estimate as for the 1 hour time step were used. The descriptive statistics may be found in Tables 2.14 and 2.15 and comparative statistics in Tables 2.16 and Table 2.17.

Raw radar estimates hardly exceed 20 mm, only a few times in H0203. They never exceed 30 mm, whereas the raingauge exceed those thresholds for a number of days (between 3 and 17 occurrences).

Radar data always show negative bias, except when corrected with A_{S2} adjustment factor (T31 and T101). A_{S3}, used with T32 and T102 also optimises MSE and Nash.

The correlation coefficients are higher than for the 15 minutes and 1 hour accumulations (between 0.83 and 0.91).

Similarly to the observation for the 1 hour accumulations, the occurrences of "radar detects/raingauge does not detect" are fewer than the opposite case for most locations, except for T9, T101 and T102. The accumulations over longer periods reduces the effect of time shift due to the time of fall of the hydromoeteors.

Again, the results for the validation year are better than those for the calibration year. The best data are the T32 and T102 in terms of MSE and Nash, and the T31 and T101 in terms of Bias (MRs).

2.5 Conclusion

A number of different methods for calculating adjustment factors, including a new one derived here (A_{S3}), were compared using raw radar and raingauge rainfall estimates. They are similar in magnitude between the calibration year and the validation year. It is reasonable to always use the adjustment factors computed for the calibration year. Adjustment factor A_{S3} is much smaller than the other ones. It optimises the mean square error but does not correct for the total volumes of rainfall. It is derived to minimise the mean square error and is more adapted to flood forecasting (for peaks) than for water resources management. In general, other adjustment factors values are in the range found in the literature.

Different types of precipitation estimates are defined. They are used for direct comparison. They are also used subsequently as inputs to hydrological models.

From the tables of statistics, it can be observed that the raw radar measurements always underestimate the raingauge measurements. This is usually true when using weather radar. The further from the radar location, the more the radar underestimates the rainfall. In mountainous areas, partial or total beam interception is a cause of underestimation. Vertical profiles of reflectivity are another main source of error in radar rainfall estimation.

There is variability in the rainfall yearly amounts within the Dargle catchment. Djouce raingauge recorded more rainfall than Stone, Powerscourt and Bray. The orography explains this observation.

For the 15 minutes accumulations only, the number of situations when "radar detects

/ raingauge does not detect" are more numerous than the number of situations for the opposite case. This can be explained by the time of transit of the hydrometeors between the altitude of 1000 m above ground and the ground level. Wind could also be a explanation.

The overall statistics are better for the calibration year than for the validation year. Year 2003/2004 was drier than year 2002/2003 by 30% and this is a possible reason.

Loc.		Statistics							
	Type	Sum	Mean	StDev	Min	Max	N(0.5)	N(1.0)	N(2.0)
Dj01	T1	1569.8	0.048	0.193	0.00	5.60	991	209	39
	T2	525.36	0.016	0.078	0.00	2.17	167	37	1
	T31	1599.5	0.049	0.238	0.00	6.63	990	380	95
	T32	860.9	0.026	0.128	0.00	3.57	444	112	18
Po02	T1	1343.2	0.041	0.168	0.00	8.40	725	165	22
	T2	523.8	0.016	0.078	0.00	2.12	180	29	1
	T31	1364.9	0.041	0.202	0.00	5.55	860	332	56
	T32	774.76	0.024	0.115	0.00	3.14	377	81	9
St03	T1	1407.4	0.043	0.187	0.00	5.80	861	188	42
	T2	439.9	0.013	0.067	0.00	1.65	120	24	0
	T31	1423.4	0.043	0.217	0.00	5.36	901	346	76
	T32	866.9	0.026	0.132	0.00	3.25	468	120	20
Br04	T1	1245.9	0.038	0.162	0.00	3.60	760	171	20
	T2	555.0	0.017	0.089	0.00	3.07	213	45	6
	T31	1246.8	0.038	0.199	0.00	6.91	771	278	49
	T32	660.5	0.02	0.105	0.00	3.66	300	61	10

Table 2.6: Descriptive statistics for rainfall estimates, calibration year, 15 minutes accumulations mm.

Loc.		Statistics							
	Type	Sum	Mean	StDev	Min	Max	N(0.5)	N(1.0)	N(2.0)
Dj01	T1	1112.6	0.034	0.159	0.00	3.80	679	193	13
	T2	387.1	0.012	0.064	0.00	1.55	118	17	0
	T31	1178.6	0.036	0.194	0.00	4.72	749	285	66
	T32	634.4	0.019	0.104	0.00	2.54	329	74	4
Po02	T1	920.9	0.028	0.154	0.00	6.40	548	135	24
	T2	376.9	0.011	0.071	0.00	3.48	142	21	2
	T31	982.1	0.030	0.184	0.00	9.07	575	232	48
	T32	557.5	0.017	0.104	0.00	5.14	291	72	7
St03	T1	1069.5	0.033	0.164	0.00	5.40	599	180	23
	T2	370.4	0.011	0.064	0.00	2.04	105	23	1
	T31	1198.5	0.037	0.207	0.00	6.60	722	280	71
	T32	729.9	0.022	0.126	0.00	4.01	377	105	23
Br04	T1	732.2	0.022	0.133	0.00	5.80	441	102	11
	T2	346.3	0.011	0.067	0.00	2.17	137	29	1
	T31	777.7	0.024	0.151	0.00	4.89	438	170	38
	T32	412.1	0.013	0.080	0.00	2.59	188	41	2

Table 2.7: Descriptive statistics for rainfall estimates, validation year, 15 minutes accumulations *mm*.

Loc.		Statistics									
	Type	MRs	RsMx	RsMn	MSE	MAE	Nash	Cor	r1g1	r1g0	r0g1
Dj01	T2	-0.032	1.15	-5.29	0.025	0.039	0.33	0.64	2272	1265	1259
	T31	0.001	5.43	-4.65	0.035	0.045	0.06	0.64	2272	1265	1259
	T32	-0.021	2.37	-5.09	0.022	0.038	0.40	0.64	2272	1265	1259
Po02	T2	-0.025	1.45	-7.64	0.017	0.032	0.38	0.66	2390	1163	1575
	T31	0.001	4.10	-6.41	0.024	0.037	0.14	0.66	2390	1163	1575
	T32	-0.017	2.24	-7.27	0.016	0.031	0.43	0.66	2390	1163	1575
St03	T2	-0.029	0.70	-5.50	0.023	0.035	0.34	0.69	2150	1252	1102
	T31	0.001	3.70	-4.82	0.026	0.038	0.25	0.69	2150	1252	1102
	T32	-0.016	1.96	-5.21	0.019	0.033	0.46	0.69	2150	1252	1102
Br04	T2	-0.021	1.95	-3.27	0.016	0.031	0.38	0.64	2158	1418	1118
	T31	0.000	5.12	-3.27	0.025	0.035	0.05	0.63	2158	1418	1118
	T32	-0.018	2.32	-3.27	0.016	0.031	0.39	0.64	2158	1418	1118

Table 2.8: Comparative statistics for rainfall estimates, calibration year, 15 minutes accumulations *mm*.

Loc.		Statistics									
	Type	MRs	RsMx	RsMn	MSE	MAE	Nash	Cor	r1g1	r1g0	r0g1
Dj01	T2	-0.022	1.32	-2.91	0.016	0.028	0.36	0.67	1719	992	858
	T31	0.002	4.45	-2.09	0.021	0.031	0.16	0.67	1719	992	858
	T32	-0.014	2.30	-2.60	0.014	0.026	0.45	0.67	1719	992	858
Po02	T2	-0.016	3.27	-3.97	0.013	0.022	0.43	0.71	1568	1010	555
	T31	0.002	8.87	-3.30	0.017	0.024	0.27	0.71	1568	1010	555
	T32	-0.011	4.94	-3.67	0.012	0.021	0.50	0.71	1568	1010	555
St03	T2	-0.021	1.44	-3.93	0.017	0.026	0.38	0.70	1700	1078	762
	T31	0.004	5.11	-2.035	0.022	0.030	0.19	0.70	1700	1078	762
	T32	-0.010	3.03	-2.51	0.014	0.025	0.48	0.70	1700	1078	762
Br04	T2	-0.012	1.78	-4.67	0.010	0.018	0.40	0.65	1282	1123	393
	T31	0.001	4.02	-3.27	0.014	0.021	0.20	0.65	1282	1123	393
	T32	-0.010	2.13	-4.46	0.01	0.018	0.42	0.65	1282	1123	393

Table 2.9: Comparative statistics for rainfall estimates, validation year, 15 minutes accumulations mm.

Loc.		Statistics							
	Type	Sum	Mean	StDev	Min	Max	N(1.0)	N(5.0)	N(10.0)
Dj01	T1	1567.5	0.190	0.667	0.00	10.6	439	26	2
	T2	518.9	0.063	0.264	0.00	6.04	137	2	0
	T31	1582.8	0.192	0.805	0.00	18.42	468	48	7
	T32	996.3	0.121	0.507	0.00	11.60	309	13	1
	T9	541.6	0.066	0.262	0.00	6.39	126	2	0
	T101	1653.7	0.201	0.798	0.00	19.49	498	50	4
	T102	1040.6	0.126	0.502	0.00	12.27	324	12	2
Po02	T1	1338.8	0.163	0.581	0.00	12.40	387	14	2
	T2	518.0	0.063	0.264	0.00	5.38	141	2	0
	T31	1351.9	0.164	0.69	0.00	14.04	400	33	4
	T32	885.74	0.108	0.452	0.00	9.20	273	9	0
	T9	548.6	0.067	0.265	0.00	5.71	142	1	0
	T101	1433.2	0.174	0.691	0.00	14.9	430	36	2
	T102	938.6	0.114	0.453	0.00	9.76	287	9	0
St03	T1	1407.4	0.171	0.640	0.00	11.60	389	19	4
	T2	439.5	0.053	0.227	0.00	3.94	113	0	0
	T31	1424.1	0.173	0.734	0.00	12.77	422	35	6
	T32	971.3	0.118	0.501	0.00	8.70	308	13	0
	T9	468.7	0.061	0.244	0.00	4.54	124	0	0
	T101	1616.9	0.196	0.790	0.00	14.72	470	49	7
	T102	1103.0	0.134	0.539	0.00	10.04	338	17	1
Br04	T1	1242.4	0.151	0.564	0.00	10.60	373	12	1
	T2	555.9	0.068	0.298	0.00	7.26	145	2	0
	T31	1250.8	0.152	0.67	0.00	16.33	375	24	5
	T32	783.8	0.095	0.420	0.00	10.23	235	10	1
	T19	610.4	0.074	0.257	0.00	4.53	142	0	0
	T101	1396	0.170	0.578	0.00	10.19	402	21	2
	T102	866.2	0.105	0.362	0.00	6.39	227	2	0

Table 2.10: Descriptive statistics for rainfall estimates, calibration year, 60 minutes accumulations mm.

Loc.		Statistics							
	Type	Sum	Mean	StDev	Min	Max	N(1.0)	N(5.0)	N(10.0)
Dj01	T1	1112.5	0.136	0.553	0.00	9.60	313	22	0
	T2	382.0	0.047	0.216	0.00	3.90	93	0	0
	T31	1165.2	0.142	0.657	0.00	11.89	359	37	3
	T32	733.5	0.090	0.414	0.00	7.48	234	6	0
	T9	372.9	0.046	0.200	0.00	3.24	97	0	0
	T101	1138.9	0.139	0.610	0.00	9.87	345	23	0
	T102	716.6	0.088	0.384	0.00	6.22	218	5	0
Po02	T1	920.8	0.112	0.505	0.00	11.80	257	15	1
	T2	372.8	0.046	0.229	0.00	5.66	99	1	0
	T31	973.1	0.119	0.598	0.00	14.77	282	28	2
	T32	637.5	0.078	0.392	0.00	9.67	178	6	0
	T9	360.3	0.044	0.198	0.00	3.32	94	0	0
	T101	941.6	0.115	0.517	0.00	8.66	273	16	0
	T102	616.7	0.075	0.338	0.00	5.57	178	3	0
St03	T1	1065.8	0.130	0.557	0.00	12.60	301	19	2
	T2	363.9	0.044	0.210	0.00	4.10	76	0	0
	T31	1179.3	0.144	0.679	0.00	13.28	361	38	6
	T32	804.3	0.098	0.463	0.00	9.06	250	11	0
	T9	415.0	0.051	0.197	0.00	3.58	83	0	0
	T101	1320.8	0.161	0.638	0.00	11.61	383	25	2
	T102	903.5	0.110	0.435	0.00	7.92	269	11	0
Br04	T1	732.2	0.089	0.434	0.00	8.40	217	7	0
	T2	341.9	0.042	0.220	0.00	3.94	82	0	0
	T31	769.3	0.094	0.494	0.00	8.86	215	21	0
	T32	482.0	0.059	0.310	0.00	5.55	128	2	0
	T9	384.8	0.047	0.198	0.00	3.19	84	0	0
	T101	886.3	0.108	0.446	0.00	7.17	235	14	0
	T102	547.3	0.067	0.280	0.00	4.49	142	0	0

Table 2.11: Descriptive statistics for rainfall estimates, validation year, 60 minutes accumulations mm.

Loc.		Statistics									
	Type	MRs	RsMx	RsMn	MSE	MAE	Nash	Cor	r1g1	r1g0	r0g1
Dj01	T2	-0.127	2.36	-8.98	0.271	0.144	0.39	0.74	976	308	587
	T31	0.002	13.42	-8.12	0.301	0.151	0.32	0.74	976	308	587
	T32	-0.694	6.59	-8.59	0.208	0.131	0.53	0.74	976	308	587
	T9	-0.124	2.61	-8.84	0.264	0.142	0.41	0.76	1165	598	398
	T101	0.101	12.49	-7.68	0.271	0.148	0.39	0.76	1214	728	349
	T102	-0.064	5.27	-8.32	0.192	0.128	0.57	0.76	1201	676	362
Po02	T2	-0.099	3.66	-9.48	0.185	0.118	0.45	0.76	1015	275	678
	T31	0.002	11.16	-4.78	0.206	0.126	0.39	0.76	1015	275	678
	T32	-0.055	6.97	-7.40	0.147	0.109	0.57	0.76	1015	275	678
	T9	-0.096	2.72	-10.50	0.183	0.116	0.459	0.76	1231	527	462
	T101	0.011	7.90	-7.44	0.203	0.124	0.39	0.76	1286	664	407
	T102	-0.048	4.65	-9.15	0.144	0.107	0.57	0.76	1261	604	432
St03	T2	-0.117	1.30	-10.34	0.253	0.131	0.38	0.76	952	323	480
	T31	0.002	8.21	-7.96	0.232	0.134	0.43	0.76	952	323	480
	T32	-0.053	4.71	-9.06	0.174	0.117	0.57	0.76	952	323	480
	T9	-0.110	2.12	-10.45	0.249	0.128	0.39	0.74	1108	625	324
	T101	0.025	9.63	-8.32	0.281	0.146	0.31	0.74	1161	793	271
	T102	-0.037	5.66	-9.30	0.187	0.120	0.54	0.74	1151	751	281
Br04	T2	-0.0834	3.36	-8.38	0.171	0.110	0.46	0.72	947	369	418
	T31	0.001	9.53	-5.60	0.222	0.121	0.30	0.72	947	369	418
	T32	-0.056	5.15	-7.47	0.156	0.107	0.51	0.72	947	369	418
	T9	-0.077	2.89	-8.28	0.163	0.112	0.49	0.78	1301	4942	64
	T101	0.019	6.50	-5.37	0.142	0.126	0.55	0.78	1332	6362	33
	T102	-0.046	4.07	-7.32	0.132	0.108	0.59	0.78	1320	5821	45

Table 2.12: Comparative statistics for rainfall estimates, calibration year, 60 minutes accumulations mm.

Loc.		Statistics									
	Type	MRs	RsMx	RsMn	MSE	MAE	Nash	Cor	r1g1	r1g0	r0g1
Dj01	T2	-0.089	2.42	-7.18	0.177	0.102	0.42	0.77	768	251	408
	T31	0.006	9.84	-4.52	0.180	0.106	0.42	0.77	768	251	408
	T32	-0.046	5.75	-5.00	0.128	0.091	0.59	0.77	768	251	408
	T9	-0.009	1.41	-6.97	0.179	0.102	0.42	0.79	900	514	276
	T101	0.003	5.94	-4.76	0.145	0.098	0.53	0.79	937	662	239
	T102	-0.048	3.30	-5.22	0.120	0.088	0.61	0.79	922	606	254
Po02	T2	-0.067	1.32	-8.32	0.124	0.078	0.52	0.81	727	258	278
	T31	0.006	7.97	-5.83	0.123	0.078	0.52	0.81	727	258	278
	T32	-0.034	3.13	-6.51	0.089	0.068	0.65	0.81	727	258	278
	T9	-0.068	1.28	-8.97	0.137	0.083	0.47	0.81	830	606	175
	T101	0.002	4.52	-5.99	0.010	0.076	0.61	0.81	860	865	145
	T102	-0.037	2.20	-7.38	0.094	0.068	0.63	0.81	846	746	159
St03	T2	-0.085	1.99	-8.50	0.176	0.096	0.43	0.79	780	264	331
	T31	0.014	9.52	-4.61	0.171	0.100	0.45	0.79	780	264	331
	T32	-0.032	5.66	-4.83	0.116	0.084	0.62	0.79	780	264	331
	T9	-0.079	0.98	-9.88	0.178	0.098	0.43	0.81	949	3231	162
	T101	0.031	5.93	-4.18	0.145	0.110	0.53	0.81	971	3399	140
	T102	-0.020	3.15	-6.59	0.109	0.089	0.65	0.81	967	3341	144
Br04	T2	-0.048	3.22	-5.30	0.094	0.062	0.50	0.76	625	318	162
	T31	0.004	7.24	-4.57	0.108	0.068	0.43	0.76	625	318	162
	T32	-0.031	4.54	-4.84	0.082	0.059	0.57	0.76	625	318	162
	T9	-0.042	1.56	-6.16	0.101	0.067	0.47	0.74	727	3179	60
	T101	0.019	5.00	-4.60	0.099	0.083	0.48	0.74	758	4816	29
	T102	-0.023	2.46	-5.65	0.086	0.067	0.55	0.75	745	3990	42

Table 2.13: Comparative statistics for rainfall estimates, validation H0304, 60 minutes accumulations mm.

Loc.		Statistics							
	Type	Sum	Mean	StDev	Min	Max	N(10)	N(20)	N(30)
Dj01	T1	1567.5	4.570	8.467	0.00	58.40	56	18	11
	T2	518.9	1.513	2.883	0.00	18.20	12	0	0
	T31	1582.7	4.614	8.794	0.00	55.51	53	23	14
	T32	1380.4	4.024	7.669	0.00	48.41	49	19	9
	T9	541.6	1.579	2.989	0.00	18.18	14	0	0
	T101	1653.7	4.8221	9.121	0.00	55.47	53	24	14
	T102	1440.7	4.200	7.950	0.00	48.36	47	19	8
Po02	T1	1338.8	3.903	7.737	0.00	55.00	43	14	7
	T2	518.0	1.510	2.994	0.00	20.80	11	1	0
	T31	1351.9	3.942	7.814	0.00	54.30	43	18	8
	T32	1258.7	3.670	7.275	0.00	50.54	42	17	5
	T9	548.6	1.599	3.118	0.00	21.48	11	2	0
	T101	1433.2	4.178	8.141	0.00	56.08	46	19	9
	T102	1333.1	3.887	7.578	0.00	52.19	42	17	9
St03	T1	1407.4	4.103	8.151	0.00	61.80	43	17	8
	T2	439.5	1.281	2.619	0.00	20.84	5	1	0
	T31	1424.1	4.152	8.484	0.00	67.52	43	18	10
	T32	1257.1	3.665	7.489	0.00	59.60	37	16	5
	T9	4989.7	1.454	2.899	0.00	19.87	12	0	0
	T101	1616.9	4.714	9.397	0.00	64.45	51	19	13
	T102	1426.2	4.158	8.292	0.00	56.83	43	19	11
Br04	T1	1242.4	3.622	7.383	0.00	52.54	44	13	7
	T2	555.9	1.621	3.214	0.00	26.52	13	1	0
	T31	1250.8	3.647	7.232	0.00	59.57	43	16	6
	T32	1134.0	3.306	6.557	0.00	54.10	37	13	3
	T9	610.4	1.780	3.009	0.00	21.53	9	1	0
	T101	1395.9	4.070	6.769	0.00	48.55	41	16	6
	T102	1245.2	3.630	6.137	0.00	43.92	37	10	3

Table 2.14: Descriptive statistics for rainfall estimates, calibration year, 1 day accumulations mm.

Loc.		Statistics							
	Type	Sum	Mean	StDev	Min	Max	N(10)	N(20)	N(30)
Dj01	T1	1112.6	3.263	6.603	0.00	57.20	33	10	4
	T2	382.0	1.1210	2.337	0.00	15.94	6	0	0
	T31	1165.2	3.417	7.127	0.00	48.62	35	13	6
	T32	1016.2	2.980	6.216	0.00	42.40	29	12	4
	T9	372.9	1.094	2.222	0.00	14.06	5	0	0
	T101	1138.9	3.340	6.775	0.00	42.90	36	11	5
	T102	991.9	2.909	5.910	0.00	37.40	31	10	5
Po02	T1	920.6	2.700	5.521	0.00	40.60	29	8	3
	T2	372.8	1.093	2.368	0.00	17.26	7	0	0
	T31	973.8	2.854	6.180	0.00	45.05	26	9	6
	T32	905.9	2.657	5.754	0.00	41.94	25	9	5
	T9	360.2	1.057	2.212	0.00	14.29	7	0	0
	T101	941.65	2.761	5.771	0.00	37.33	26	9	5
	T102	875.49	2.567	5.375	0.00	34.72	25	9	3
St03	T1	1065.8	3.126	6.232	0.00	46.00	26	9	5
	T2	363.9	1.067	2.114	0.00	14.16	5	0	0
	T31	1179.3	3.458	6.850	0.00	45.87	38	13	5
	T32	1040.9	3.053	6.046	0.00	40.49	32	8	3
	T9	415.0	1.217	2.120	0.00	14.05	4	0	0
	T101	1320.7	3.875	6.886	0.00	45.51	36	13	7
	T102	1186.9	3.481	6.065	0.00	40.20	29	10	4
Br04	T1	732.2	2.147	4.699	0.00	40.80	20	5	2
	T2	341.9	1.003	2.237	0.00	19.74	5	0	0
	T31	769.2	2.256	5.034	0.00	44.41	17	6	4
	T32	697.5	2.045	4.564	0.00	40.27	13	5	1
	T9	384.8	1.128	2.215	0.00	18.18	7	0	0
	T101	886.3	2.599	4.985	0.00	40.98	18	9	1
	T102	784.9	2.302	4.519	0.00	37.09	16	7	1

Table 2.15: Descriptive statistics for rainfall estimates, validation year, 1 day accumulations mm.

Loc.		Statistics									
	Type	MRs	RsMx	RsMn	MSE	MAE	Nash	Cor	r1g1	r1g0	r0g1
Dj01	T2	-3.057	2.16	-44.16	46.498	3.138	0.34	0.88	189	10	50
	T31	0.004	25.48	-18.92	18.595	2.134	0.73	0.88	189	10	50
	T32	-0.545	21.02	-21.10	17.054	2.049	0.76	0.88	189	10	50
	T9	-2.990	1.57	-41.32	44.121	3.069	0.38	0.90	203	17	36
	T101	0.251	21.72	-21.89	16.503	2.026	0.77	0.90	204	22	35
	T102	-0.369	17.72	-23.66	14.373	1.898	0.79	0.90	203	17	36
Po02	T2	-2.393	2.06	-38.80	31.690	2.492	0.46	0.92	187	12	49
	T31	0.038	13.62	-13.69	9.219	1.565	0.84	0.92	187	12	49
	T32	-0.233	11.40	-15.63	8.844	1.498	0.85	0.92	187	12	49
	T9	-2.303	2.33	-38.30	30.063	2.413	0.49	0.93	199	20	37
	T101	0.275	16.20	-13.48	9.334	1.532	0.84	0.93	202	25	34
	T102	-0.016	14.35	-14.68	8.491	1.455	0.86	0.93	199	20	37
St03	T2	-2.821	1.64	-43.82	43.000	2.898	0.35	0.89	185	13	36
	T31	0.049	19.34	-21.12	14.769	1.926	0.78	0.89	185	13	36
	T32	-0.438	15.82	-21.90	13.565	1.841	0.79	0.89	185	13	36
	T9	-2.649	1.67	-42.84	39.451	2.747	0.40	0.90	195	21	26
	T101	0.610	23.73	-20.98	17.928	2.091	0.73	0.90	199	28	22
	T102	0.055	19.63	-21.85	14.144	1.849	0.79	0.90	195	21	26
Br04	T2	-2.001	4.78	-26.07	26.935	2.239	0.50	0.88	175	29	24
	T31	0.024	16.50	-18.15	12.621	1.744	0.76	0.88	175	29	24
	T32	-0.316	13.56	-19.04	12.200	1.703	0.77	0.88	175	29	24
	T9	-1.843	4.44	-31.01	26.613	2.197	0.51	0.91	196	142	3
	T101	0.447	13.55	-16.86	9.898	1.808	0.82	0.91	196	143	3
	T102	0.008	10.72	-18.82	9.986	1.701	0.82	0.91	196	142	3

Table 2.16: Comparative statistics for rainfall estimates, calibration year, 1 day accumulations mm.

Loc.		Statistics									
	Type	MRs	RsMx	RsMn	MSE	MAE	Nash	Cor	r1g1	r1g0	r0g1
Dj01	T2	-2.142	3.58	-43.98	26.577	2.213	0.41	0.88	173	22	43
	T31	0.154	23.81	-18.07	12.010	1.608	0.73	0.88	173	22	43
	T32	-0.282	17.60	-22.03	10.444	1.500	0.769	0.88	173	22	43
	T9	-2.169	3.52	-43.25	27.180	2.240	0.39	0.89	181	38	35
	T101	0.077	18.10	-18.48	10.211	1.513	0.77	0.89	187	45	29
	T102	-0.353	12.60	-20.09	9.478	1.447	0.79	0.89	181	38	35
Po02	T2	-1.606	1.56	-26.70	14.959	1.672	0.53	0.91	167	20	26
	T31	0.153	18.01	-11.92	6.885	1.185	0.78	0.91	167	20	26
	T32	-0.042	15.29	-12.54	6.041	1.146	0.81	0.91	167	20	26
	T9	-1.643	1.78	-28.64	15.786	1.706	0.50	0.91	176	42	17
	T101	0.061	12.47	-11.20	5.701	1.129	0.82	0.91	182	52	11
	T102	-0.132	10.71	-11.53	5.297	1.09	0.83	0.91	176	42	17
St03	T2	-2.058	0.90	-37.12	24.491	2.102	0.38	0.87	175	20	32
	T31	0.333	23.29	-24.60	11.336	1.527	0.71	0.87	175	20	32
	T32	-0.073	17.98	-24.88	9.614	1.389	0.76	0.87	175	20	32
	T9	-1.901	1.30	-34.23	23.521	2.054	0.40	0.89	191	76	16
	T101	0.747	15.31	-24.88	10.771	1.753	0.73	0.89	193	84	14
	T102	0.355	11.41	-25.11	8.802	1.621	0.78	0.89	191	76	16
Br04	T2	-1.144	3.82	-30.72	11.015	1.255	0.54	0.83	159	22	16
	T31	0.108	20.81	-18.12	8.369	1.147	0.65	0.83	159	22	16
	T32	-0.101	16.67	-20.23	7.504	1.070	0.69	0.83	159	22	16
	T9	-1.012	2.61	-28.20	10.229	1.271	0.58	0.85	173	125	2
	T101	0.452	17.38	-14.75	7.131	1.271	0.70	0.85	175	156	0
	T102	0.154	13.48	-15.69	6.261	1.164	0.74	0.85	173	125	2

Table 2.17: Comparative statistics for rainfall estimates, validation year, 1 day accumulations mm.

Chapter 3

Root Methods in flood analysis

3.1 Introduction

A number of difficulties often arise in relation to the estimation of effective precipitation for the purpose of flood prediction using linear models. These include (a) the uncertainties in estimating areal precipitation accurately, (b) the uncertainties in relation to the initial soil moisture conditions in the catchment, (c) the reduction of total precipitation to effective precipitation due to evaporation, infiltration and groundwater recharge. Errors in the unit-hydrograph derived from past storms due to such factors will affect the procedure adopted for flood forecasting in real-time. This situation suggests the investigation of the usefulness of these methods which have been developed to derive the unit-hydrograph without reference to rainfall data. Of particular interest in this connection is the root selection method (Turner et al., 1989).

This chapter describes a preliminary study of this question. A description of the unit-hydrograph may be found in Chapter **??**. In the following, descriptions are given of the principal alternative methods. The ARMAX method is presented first, before other methods which are independent of the rainfall data. They include the original root-matching method of de Laine (1970, 1975), the root selection method due to Turner (1982) and the FDTF-ERUHDIT method (Duband et al., 1993) which derives both the unit-hydrograph and the loss function by alternate successive deconvolutions which converge to a solution, the loss function defining the conversion from total rainfall into effective rainfall. A new method was developed and is presented here. A number of numerical experiments were carried out

using synthetic data based on simple arrangements of linear reservoirs in order to validate the new method and the computer program used. The root selection method was then applied to actual storm floods on the Dargle catchment.

3.2 The ARMAX Method

The auto-regressive moving average method (ARMA) is a classical method for the analysis of time series analysis of discharge data (Box and Jenkins, 1976). This is the stochastic equivalent of the deterministic least squares approach represented by Equation (**??**) above. The ARMA approach was extended by Gouy (1991) to allow for exogenous input in the case of catchment response. That method, referred to as ARMAX (AutoRegressive Moving Average with eXogenous input), has been first presented by Gouy (1991) in an attempt to develop a method of deriving the unit-hydrograph by employing the polynomial formulation suggested by de Laine (see 3.3.2). It requires flow and rainfall data and methods of derivation of excess rainfall and direct runoff.

Assuming the relationship between direct runoff (output) and effective rainfall (input) as linear, as for the unit hydrograph approach, a catchment rainfall-runoff model may be developed using the ARMAX(p, q) formulation as follow:

$$y_\kappa + \sum_{i=1}^{i=p} a_i \, y_{\kappa-i} = \sum_{j=0}^{j=q} b_j \, x_{\kappa-j} + e_\kappa \tag{3.1}$$

where:

- y_κ is the direct runoff (output),
- x_κ is the effective rainfall (input),
- e_κ is the error,
- κ is the timestep index,
- a_i are the coefficients of the autoregressive part (order p; direct runoff),
- b_j are the coefficients of the moving average on the exogenous input part (order q; excess rainfall).

Taking the z-transform of Equation (3.1) gives:

$$Y(z^{-1}) + \sum_{i=1}^{i=p} \left[a_i \, z^{-i} \, Y(z^{-1})\right] = \sum_{j=0}^{j=q} \left[b_j \, z^{-j} X(z^{-1})\right] + E(z^{-1}) \tag{3.2}$$

which can also be written as:

$$Y(z^{-1})\left[1 + A(z^{-1})\right] = X(z^{-1})B(z^{-1}) + E(z^{-1}) \tag{3.3}$$

where:

$$A(z^{-1}) = \sum_{i=1}^{i=p} (a_i z^{-i}) \tag{3.4}$$

$$B(z^{-1}) = \sum_{i=1}^{i=q} (b_j z^{-j}) \tag{3.4'}$$

The z-transform of the convolution product in Equation (**??**) is:

$$Y(z^{-1}) = H(z^{-1})X(z^{-1}) \tag{3.5}$$

By comparing Equations (3.3) and (3.5), we can identify the transfer function of the system as:

$$H(z^{-1}) = B(z^{-1}) / \left[1 + A(z^{-1})\right] \tag{3.6}$$

In order to obtain that transfer function, an ARMAX model of a suitable order has to be fitted. To do so, some assumptions have to be made regarding the methods of baseflow component separation and effective rainfall derivation. Then, we may compute the polynomial division above (Equation (3.6)) following the ascending powers and finally normalize the coefficients. Multi-event data are recommended for this method, which is equivalent to finding a Padé approximation to $H(z^{-1})$, as we produce a rational-fraction approximation with the form $Y(z^{-1})/X(z^{-1})$.

If needed, the same formulation allows us to compute some missing effective rainfall series by using:

$$X(z^{-1}) = Q(z^{-1})\left[1 + A(z^{-1})\right] / B(z^{-1}) \tag{3.7}$$

The coefficients obtained are then normalized and multiplied by the total volume of runoff to get the series of effective rainfall.

By dividing the polynomials following the ascending powers, the series length is not limited by a mathematical constraint any more. This division can be processed up to any

preferred exponent. Many examples of application of the method may be found in the thesis by Gouy (1991). The ARMAX approach has two main advantages, (1) it is simple and (2) it does not require constraints, since the polynomial division can be carried out up to any chosen degree with no limits on the duration of the unit-hydrograph.

3.3 Rainfall independent methods

There is often a mismatch between the accuracy of areal rainfall estimates and discharge. Discharge is usually more accurate so that estimated precipitation is a weakness. Rainfall independent methods, by contrast with the methods presented above, do not require any rainfall data and thus make no assumptions on the derivation of effective rainfall. Hereinafter are presented three methods of that type, namely the FDTF-ERUHDIT, the Root matching and the Root selection methods.

3.3.1 The FDTF-ERUHDIT method

Basis of the method

The FDTF method (First Derivative Transfer Function) was developed in France by Duband et al. (1993) over the last fifteen years and has been applied to a number of catchments with some success for reservoir system control and management. Essentially it aims at making the whole identification process of the unit hydrograph more objective and avoiding as much as possible uncontrolled and arbitrary choices in selecting and calibrating a production function and in separating the baseflow component (Duband et al., 1993). Although it is described as requiring both rainfall data and flow data, the same method could actually be applied without knowledge of the rainfall pattern by assuming a hypothetical rainfall pattern with the correct total volume. That is why it has been classified as a "rainfall independent method" and included in this section.

A general assumption is that the UH model structure can adequately represent the catchment behaviour, that is we may assume the existence of two separately acting functions called production and transfer function respectively. It is known that the mechanisms affecting the production of effective rainfall are non-linear, so the production function should show non-linearity characteristics. If the mechanisms driving the routing of the effective

rainfall to the outlet as runoff are assumed to be linear and time-invariant, the hydrological system routing part may be modelled by a linear transfer function known as the unit hydrograph.

The immediate objective is to adapt a unique average transfer function to all events taken from a set of independent rainfall-runoff events and to obtain separately (event by event) the likely series of excess precipitation. That means two sets of unknowns (i.e. excess precipitation and transfer function) have to be identified from only one source of information (i.e. observed discharges). In practice, an alternative iterative algorithm, proposed by Newton and Vineyard (1967), is adopted since an estimate of one set of unknowns can only be derived from an estimate of the other set of unknowns. The criterion of optimality requires that these two sets combine linearly in such a way to allow optimal reproduction of the set of observed discharges. Non-uniqueness in the solution may be removed by applying plausibility constraints to the identified unknowns, for example the conservation of volumes or the ordinates positivity rules. An a priori baseflow separation technique is not required because the method works with the differentiated discharge data and this filters out the slowly varying component which is also strongly autocorrelated.

All this requires an appropriate conditioning of the data and of the equations. The equations are always expressed in their discrete form, and thus an appropriate timestep is required which is consistent with the observed dynamics of the flood events (Obled, 1989).

Say, we collect data for a certain number (NF) of flood events for a given catchment. For each event L ($L = 1, ..., NF$), the following variables are defined:

1. The gross precipitation PG, which is the best estimate of the basin averaged rainfall. There is one value of PG per timestep i of the L^{th} event: PG_i^L ($i = 1, ..., mm^L$) where mm^L is the total number of steps with measured input rainfall for the event L (i.e. non null rainfall). m^L denotes the total duration of the rainfall in the event L,

2. The discharge at the basin outlet Q_i^L, over p^L timesteps. For the event L, this total length p^L corresponds to m^L plus the n timesteps for the recession minus one. n is thus the duration of the unit-hydrograph $\mathbf{h}$, and it has to be chosen a priori. In addition, the starting time of the event is defined as the time when the discharge starts to rise.

Furthermore, the absolute value of the discharge will not be used. In order to avoid baseflow separation, we work on first differences, as suggested by Guillot and Duband (1980). Substracting two time steps in sequence, and calling $q_i^L = Q_i^L - Q_{i-1}^L$ the discharge variation between steps $(i-1)$ and (i), then:

$$q_i^L = \sum_{j=1}^{j=n+1} H_j \, PE_{i-j+1}^L + \left(Q_{B_i}^L - Q_{B_{i-1}}^L\right) \tag{3.8}$$

is the typical unit-hydrograph convolution equation, as described in section **??**. Subscript B denotes the baseflow component.

H_j is the first difference transfer function (FDTF), defined as:

$$H_1 = h_1, \; H_j = (h_j - h_{j-1}) \text{ for } j = 2, ..., n \text{ and } H_{n+1} = -h_n$$

If we assume that the baseflow first difference is negligible, since that component is slowly varying with time, Equation (3.8) may be rewritten as:

$$q_i^L \approx \sum_{j=1}^{j=n+1} H_j \, PE_{i-j+1}^L \tag{3.9}$$

The later equation is valid at least for the rising limb and the first part of the recession limb of the unit-hydrograph. It also provides a partial whitening of the discharge series, as discharge increments are much less auto-correlated than the discharges themselves. This will prove useful in any identification technique used afterwards, although it has the disadvantage that differentiating tends to amplify any random error noise.

Moreover, if the absolute value of the discharge data is affected by a systematic error such as a shift in the recorded level or in the rating curve, the differentiated value is much less sensitive to these errors.

Once this data set is prepared, the identification of the two sets of unknowns, namely the transfer function vector $\mathbf{h}$ and the vectors $\mathbf{PE}^L$ related to the excess precipitation PE_i^L may begin.

The method starts by assuming any acceptable pattern for the effective rainfall. It then repeats two steps until a satisfactory estimate is obtained. In the first step the transfer function is estimated using the flow data and the current estimate of the excess rainfall. In the second step the excess rainfall is estimated using the flow data and the current estimate of the transfer function. Both steps involve deconvolution and are described below.

In practice, the gross precipitation can be used as an initial estimate of the excess precipitation, i.e:

$$PE_i^L\{0\} \approx PG_i^L \tag{3.10}$$

where $PE_i^L\{k\}$ denotes the k^{th} estimate of PE_i^L (at the k^{th} iteration).

Transfer function identification

Equation (3.9) written out for all the p^L timesteps of each event, provides for the NF events an over determined linear system of n^{tot} equations and n unknowns, with:

$$n^{tot} = \sum_{L=1}^{L=NF} p^L \tag{3.11}$$

as the total number of discharges ordinates available, and therefore the total number of equations used to solve for the transfer function.

Several methods of identification of the transfer function are now available to compute the transfer function. Among these are the Least-Squares, the Ridge regression (Bruen and Dooge, 1984), or the ARMAX method previously described in section 3.2. Any of these methods could be used. Here we use the ARMAX method fitted with recursive least-squares and maximum likelihood algorithms.

Some constraints are to be applied to the identified transfer function in order to ensure the positiveness of the unit-hydrograph ordinate and also the conservation of the volume of water when transferred from excess rainfall to runoff. Those constraints could be included in the least squares algorithm through a Lagrange multiplier (Versiani, 1983; Wormleaton, 1980). However, by it is preferred here to apply the constraints a posteriori to an a priori unconstrained solution. At the end of the present k step in the global algorithm, an estimate of the unit-hydrograph is available.

Effective rainfall deconvolution

The deconvolution of effective precipitation, in other words the computation of the excess precipitation at step k, is based on Equation (3.9) in which the unknowns are now the PE_j^L which can also be written as a vector $\mathbf{PE}^L$. The solution may be computed event by event.

For event L, the system of equations is again over determined. There are mm^L unknown effective rainfall to identify, and $p^L = m^L + n - 1$ equations are available. This allows at

least $n-1$ degrees of freedom, whatever the number of unknowns mm^L.

The least-squares method could be applied in this case, and the solution would be:

$$\mathbf{PE}^L = \left[\mathbf{F}^T\mathbf{F}\right]^{-1}\mathbf{F}^T\mathbf{q}^L \tag{3.12}$$

This problem is often ill-conditioned, and instability in the solution $\mathbf{PE}^L$ may be commonly observed. For that reason, the ridge regression method with least-squares (Hoerl and Kennard, 1970), also referred to as smoothed least-squares, is preferred because of the strong collinearity between equations. It was not necessary when computing the transfer function because of the large number of events available then. The idea underlying the ridge regression method consists in reinforcing the diagonal of the matrix to be inverted (here $\mathbf{F}^T\mathbf{F}$) in such a way as to improve its numerical conditioning by making it more similar to a fully diagonal matrix (refer to section **??**). The initial system is changed, and thus, the solution is slightly biased, but on the other hand, the sampling variability of the estimated variables (here $\mathbf{PE}^L$) is significantly reduced (Bruen and Dooge, 1984).

The usual least-squares equation becomes now:

$$\mathbf{PE}^L = \left[\mathbf{F}^T\mathbf{F} + \gamma(k)\,\mathbf{Diag}\left(\mathbf{F}^T\mathbf{F}\right)\right]^{-1}\mathbf{F}^T\,\mathbf{q}^L \tag{3.13}$$

where each diagonal term is increased by a given fraction $\gamma(k)$ as low as possible and decreasing with the advancement in the iterations.

In the same way it is made for the transfer function identification, two sorts of constraints are applied to the PE_S: first, the PE_j^L are to remain positive, secondly, the excess rainfall is to remain less than the gross rainfall.

Some other techniques have been tested in order to solve the inverse problem, e.g. linear and quadratic programming (Nalbantis, 1987; Natale and Todini, 1976), or orthogonolising $\mathbf{F}^T\mathbf{F}$ (Guillot and Duband, 1980). However, no definite advantage was found over the ridge regression method.

Use and evaluation of the method

The whole FDTF identification procedure as stage A is shown as Figure3.1. In practice, three to five iterations are enough to reach convergence with a relatively high value for the convergence criterion. One may then investigate a posteriori what type of production

function could be obtained from the observed gross precipitation, with an output as close as possible to the effective precipitation identified with the FDTF method (see Stage B on Figure 3.1). The method was used for the Gardon d'Anduze in France with encouraging results (Duband et al., 1993).

Nalbantis et al. (1995) evaluated the method, which is robust against moderate departures from the assumption of a linear transfer function. It is much more robust against rainfall data errors than against discharge data errors. Although the uniqueness of the solution can not be proved theoretically, a series of computer experiments confirms such a uniqueness in practice. The use of the Ridge Regression method to derive the effective rainfall series is absolutely necessary and its smoothing parameter must be proportional to the amount of error in the data, especially the discharge data.

With such constraints on data requirements and given the usefulness of the unit hydrograph approach underlined by Jakeman et al. (1990), the FDTF-ERUHDIT method appears to be a very robust exploratory tool for identifying the transfer function and the effective rainfall series, and therefore allowing for a more objective choice and calibration of the soil moisture accounting routine.

3.3.2 The root matching method (De Laine)

This method has been suggested by de Laine (1970, 1975). It mainly differs from the classical methods to the extent that it only requires runoff data from different storms for a given catchment. The z-transform, which is actually an extension of the Fourier transform to discrete functions, is defined as:

$$F(z^{-1}) = \sum_{s=0}^{s=\infty} f(sT) z^{-s} \tag{3.14}$$

where $F(z^{-1})$ is the polynomial with coefficients equal to the corresponding ordinates of the original discrete function $f(sT)$.

After Saucedo and Schiring (1968), for a linear time-invariant system, the z-transform of the input X, the pulse response H and the output Y are connected by:

$$Y(z^{-1}) = X(z^{-1}) H(z^{-1}) \tag{3.15}$$

where Y, X and H are respectively of order p, m and n. Deriving the transfer function

by dividing the polynomial $Y(z^{-1})$ by $X(z^{-1})$ is not entirely satisfactory because of the sensitivity of the result to errors in the data.

Another use of the relationship between the three polynomials (Equation (3.15)) has been offered by De Laine. Knowing that a set of p roots of $Y(z^{-1})$ is made up of the m roots of $X(z^{-1})$ and the n roots of $H(z^{-1})$, de Laine (1970) suggested that, by examination of the outputs of two or more storms of differing characters, the common roots in the runoff polynomial could be identified as being independent of the rainfall and hence attributable only to the transfer function $h(sT)$.

An interesting point has been underlined by de Laine (1970) regarding non-linear systems and inexact data. Indeed, it is unlikely a catchment will behave as a linear system, and, on the other hand, there could be gaps and errors in the discharge time-series. In such cases, it might become much more difficult to recognize common roots. When there is no assurance about the correspondence of roots, more data sets would be required. In general, sufficient data sets should be analyzed to ensure that there is no doubt about the conclusion. When no pairing of the roots is possible, despite the availability of sufficient data sets of good accuracy, then, that would prove that the catchment behaves as a non-linear system, and therefore, the unit-hydrograph approach should be abandoned for that case.

For this method, a compromise must be found regarding the frequency of sampling of the output. Indeed, the greater the frequency of sampling, the better the definition of the system. On the other hand, the more sampling points are available, the more difficult it is to recognize pairs of roots. It would be advised to first determine a suitable frequency of the sampling for any given catchment.

A major feature of the method is that it only requires output (direct runoff) data, and does not require an estimate of effective rainfall, which is seen as a main problem when using the more usual unit-hydrograph-based approaches. In fact, the net rainfall can actually be estimated by this method. When a measurement of the precipitation is available for the event, one may compare the net rain derived from De Laine method with the one obtained from the more usual methods of effective rain estimation of effective rainfall.

Four disadvantages of the basic method were identified by Turner et al. (1989). They can be summarized as follow:

1. Common roots for the transfer function polynomials of several events can be found only if the catchment behaves as a perfect linear, time-invariant system. This is a strong assumption,

2. The roots' values are highly sensitive to the polynomial coefficient values, and hence the method is very sensitive to errors in the runoff data,

3. The method of baseflow separation chosen can have a significant effect on the values of the complex roots. When the baseflow separation is inaccurate, the values of the complex roots will contain errors,

4. The values of the complex roots for any given storm are very sensitive to the point of curtailment of the direct runoff hydrograph since the number and hence the value of the roots will vary with the duration of direct runoff assumed. The effect of this is to make root matching between two events very difficult.

3.3.3 The root selection method (Turner)

The principle of the Turner method can then be expressed as follow:
We then can identify the transfer function and the effective rainfall using only one flood event by plotting the roots of the output (direct runoff) polynomial and by considering that:

- The roots associated with the transfer function appear either as points on a "skew" circle or as points on the real axis. The remaining roots are associated with the effective rainfall.

- By comparison with the De Laine method previously described, the Turner method also allows the analysis of longer flood events, since the pattern of the roots associated with the transfer function is more discernible on an Argand diagram.

Turner (1982) applied De Laine's method to a number of historical storm events for his study of reservoir inflows on the river Liffey. The complex roots were plotted and several features were noted for the different flood events:

1. A definite relationship existed between the overall shapes of the root patterns for this particular catchment,

2. A specific skewed circular pattern of roots was common to virtually all flood hydrographs.

To evaluate the significance of these observations, experiments were carried out in which the observed root patterns were compared with the root patterns obtained for conceptual models commonly used to represent to unit-hydrograph.

We detail here the results obtained for the Nash cascade of n equal linear reservoirs of delay parameter K (Nash, 1958). The impulse unit hydrograph $h_0(t)$ is given by:

$$h_0(t) = \frac{1}{K} \frac{\exp(-t/K)(t/K)^{n-1}}{(n-1)!} \tag{3.16}$$

The T-period unit-hydrograph, denoted $h_T(t)$, for a Nash cascade of n reservoirs, each with delay time K, is given by:

$$h_T(t) = \frac{S(t) - S(t-T)}{T} \tag{3.17}$$

where:

$$S(t) = \int_0^t h_0(\tau)\, d\tau = 1 - \exp(-t/K) \sum_{i=0}^{i=n-1} \frac{t^i}{i!K^i} \tag{3.18}$$

is the S-curve due to uniform effective rainfall lasting indefinitely.

In the simple case of a single reservoir (n=1), the transfer function becomes:

$$h_0(t) = \frac{1}{K} \exp(-t/K) \tag{3.19}$$

and from Equation (3.18):

$$S(t) = 1 - \exp(-t/K) \tag{3.20}$$

with:

$$S(0) = 0 \tag{3.21}$$

$$S(T) = 1 - \exp(-T/K) \tag{3.22}$$

which gives by Equation (3.17):

$$h_T(t) = \frac{\exp(-(t-T)/K) - \exp(-t/K)}{T} \quad \text{for} \quad T \leq t \leq NT \tag{3.23}$$

which may also be written as:

$$h_T(t) = \frac{\exp(T/K) - 1}{T} \exp(-t/K) \quad \text{for} \quad T \leq t \leq NT \tag{3.24}$$

with:

$$h_T(0) = 0 \tag{3.25}$$

$$h_T(T) = \frac{1 - \exp(-T/K)}{T} \tag{3.26}$$

The sampled T-period unit hydrograph for $s \geq 1$ may be written as:

$$h_T(sT) = \frac{\exp(T/K) - 1}{T} \exp(-sT/K) \tag{3.27}$$

The z-transform of the sampled T-period unit-hydrograph of length NT is, according to Equation (3.14):

$$H(z^{-1}) = \sum_{s=0}^{s=N} h_T(sT)\, z^{-s} \tag{3.28}$$

Replacing $h_T(sT)$ with its value from Equation (3.27), we get:

$$H(z^{-1}) = \sum_{s=1}^{s=N} \frac{\exp(T/K) - 1}{T} \exp(-sT/K)\, z^{-s} \tag{3.29}$$

which may be written as:

$$H(z^{-1}) = \frac{\exp(T/K) - 1}{T} \sum_{s=1}^{s=N} \left(\exp(-T/K)\, z^{-1}\right)^s \tag{3.30}$$

Applying the formula for the sum of a geometric series to the previous equation gives:

$$H(z^{-1}) = \frac{\exp(T/K) - 1}{T} \exp(-T/K)\, z^{-1}\, \frac{1 - \left(\exp(-T/K)\, z^{-1}\right)^N}{1 - \exp(-T/K)\, z^{-1}} \tag{3.31}$$

The N roots of the z-transform of the sampled pulse response given by Equation (3.31) are:

$$z^{-1} = 0 \qquad \text{once} \tag{3.32}$$

$$z^{-1} = \exp(T/K)\, (1)^{1/N} \qquad (N-1) \text{ times} \tag{3.32'}$$

$(1)^{1/N}$ corresponding to the N complex roots of unity with exception of the positive real root which cancels the denominator. Note that the expression above (Equation (3.31)) is not indeterminate when z^{-1} takes the value $\exp(T/K)$, the proof being based on l'Hopital rule. These $(N-1)$ roots can be plotted on an Argand diagram. They describe a circle of radius $\exp(T/K)$ centered on the origin (see Figure 3.2.

For n=2, we have for the instantaneous unit-hydrograph:

$$h_0(t) = \frac{1}{K}\, (t/K) \exp(-t/K) \tag{3.33}$$

which gives:

$$S(t) = 1 - (1 + t/K)\exp(-t/K) \tag{3.34}$$

with:

$$S(0) = 0 \tag{3.35}$$

$$S(T) = 1 - (1 + T/K)\exp(-T/K) \tag{3.36}$$

The finite period unit-hydrograph is then given by:

$$h_T(t) = \frac{1}{T}\left[\left(1 + \frac{(t-T)}{K}\right)\exp(-(t-T)/K) \; - \left(1 + \frac{t}{K}\right)\exp(-t/K)\right] \quad \text{for} \quad T \le t \le NT \tag{3.37}$$

which may also be written as:

$$h_T(t) = \frac{1}{T}\left\{\exp(-t/K)\left[\exp(T/K)\left(1+\frac{(t-T)}{K}\right)-\left(1+\frac{t}{K}\right)\right]\right\} \quad \text{for} \quad T \le t \le NT \tag{3.38}$$

with:

$$h_T(0) = 0 \tag{3.39}$$

$$h_T(T) = \frac{1}{T}\left[1 - (1 + T/K)\exp(-T/K)\right] \tag{3.40}$$

The sampled T-period unit-hydrograph for $s \ge 1$ may be expressed as:

$$\begin{aligned} h_T(sT) &= \frac{1}{T}\left[\exp(T/K)\left(1 + \frac{(s-1)T}{K}\right) - \left(1 + \frac{sT}{K}\right)\right]\exp(-sT/K) \\ &= \frac{1}{K}\left[s\left(\exp(T/K) - 1\right) + \exp(T/K)\left(\frac{K}{T} - 1\right) - \frac{K}{T}\right]\exp(-sT/K) \end{aligned} \tag{3.41}$$

If the point corresponding to the start of rainfall is labelled as s=1 instead of s=0, then Equation (3.40) and (3.41) are multiplied by s and there is an additional root at s=0.

For the case of a Nash cascade of n equal linear reservoirs, it can be shown that the root pattern of the polynomial associated with the transfer function is changed in such a way that the non-zero roots are plotted on a "skew" circle and are regularly spaced. The zero root centered on the origin actually represents the unit delay at the start of the runoff to the first non-zero sampled ordinate.

Figures **??** and 3.3 describe the unit-hydrographs for both a single reservoir (K=5, n=1, N=20, T=1) and a Nash cascade of reservoirs (K=1, n=5, N=20, T=1), together with their associated roots presented on Argand diagrams.

The equivalent discrete model suggested by O'Connor (1976, 1982) will not be described here, as we concentrate later on the continuous Nash cascade model to develop our new approach as a variation on the Turner method.

Turner et al. (1989) adapted the De Laine method to a single storm case in order to derive the transfer function, this time using both input (rainfall) and output (runoff) data. The unit-hydrograph was reconstructed from the roots not related to the input polynomial. Numerical experiments indicated that for a 10% error in the data, that method would result in an average error of 7% in the unit hydrograph. That was a considerable improvement on the explosive error level of 5000% found when using polynomial division, but was still in excess of what could be achieved by using classical methods such as least-squares, orthogonal transforms or conceptual models (Dooge, 1979).

On the basis of worked examples, Turner (1982) has shown that the unit-hydrograph is largely or entirely made up of the roots on the skew circle, as expected considering the results for the conceptual models. When dealing with the "skew circle", the selection or not of individual pairs of roots does not substantially alter the overall shape of the unit-hydrograph.

3.4 A variation on the Turner method

To improve on previous methods, the roots corresponding to the rainfall are separated and the total response is then split into a quick response and a slow response. In the new method, a model structure is imposed and its parameters are the unknowns to be identified. In this method, here is no need for baseflow separation.

To illustrate the derivation, it is assumed that the quick and slow responses may be represented by single linear reservoirs in parallel with time constants K_1 and K_2 respectively. The splitting of the input between the two reservoirs is represented by a constant splitting parameter α. A parametric approach to the unit-hydrograph derivation is more robust and provides quantitative information on the catchment time delay and the rainfall loss function).

The reservoir parameters can be estimated from the average radii of the roots patterns for selected portions of ordinates of the total hydrograph. The first ordinates of the recession

of the storm runoff hydrograph, after the cessation of the effective rainfall, are used to derive the fast reservoir parameter. The long series of ordinates of the recession part, or the series of the later part of the recession are used to derive the slow reservoir parameter. The choice of the recession period considered is relatively subjective. It depends on what part of the slow recession is required to be best modeled by the slow reservoir. It is recommended that the ordinate corresponding to the start of the baseflow contribution should be used as the beginning of that period. The splitting parameter is then estimated using information on the lag between the input and the output.

The method is applied to synthetic data and analytical solutions are sought in order to validate the method and also a computer program developed to automate the operations required in the method (see chapter **??**). Those synthetic data correspond to the two component response of two linear reservoirs in parallel. The method is then applied to real data taken from storms on the Dargle catchment (see chapter **??**).

3.4.1 Analysis of a two component response

The z-transform of the unit hydrograph for a single reservoir is given by:

$$H(z^{-1}) = \left[\frac{\exp(T/K)-1}{T}\right] \exp(-T/K)z^{-1} \left\{ \frac{1-\left[\exp(-T/K)\, z^{-1}\right]^N}{1-\left[\exp(-T/K)\, z^{-1}\right]} \right\} \tag{3.42}$$

For two reservoirs in parallel, where a fraction α of the flow goes through the fast reservoir with delay parameter K_1 and the remaining $(1-\alpha)$ part of the flow goes through the slower reservoir with delay parameter K_2 ($0 \leq \alpha \leq 1$, $K_2 > K_1$, (see Figure 3.4), the z-transform of the unit-hydrograph is:

$$H(z^{-1}) = \alpha\, H_1(z^{-1}) + (1-\alpha)\, H_2(z^{-1}) \tag{3.43}$$

By substituting Equation (3.42) twice into (3.43) with the respective values of K_1 and K_2, the z-transform of the combined system can be derived as the ratio of two polynomials:

$$\begin{aligned} H(z^{-1}) = \alpha & \left[\frac{\exp(T/K_1)-1}{T}\right] \exp(-T/K_1)z^{-1} \left\{ \frac{1-[\exp(-T/K_1)z^{-1}]^N}{1-\exp(-T/K_1)z^{-1}} \right\} \\ +(1-\alpha) & \left[\frac{\exp(T/K_2)-1}{T}\right] \exp(-T/K_2)z^{-1} \left\{ \frac{1-[\exp(-T/K_2)z^{-1}]^N}{1-\exp(-T/K_2)z^{-1}} \right\} \end{aligned} \tag{3.44}$$

Setting the numerator of the above expression equal to zero, the root pattern for the two reservoirs in parallel is obtained. If the numerator of Equation (3.44) is denoted $\Lambda(z^{-1})$, it

may be written as:

$$\Lambda(z^{-1}) \;=\; A_1 \left\{1 - \left[\exp(-T/K_1)\, z^{-1}\right]^N\right\} + A_2 \left\{1 - \left[\exp(-T/K_2)\, z^{-1}\right]^N\right\} \qquad (3.45)$$

where:

$$A_1 = \alpha \left[\exp(T/K_1) - 1\right] \exp(-T/K_1) z^{-1} \left[1 - \exp(-T/K_2)\, z^{-1}\right] \qquad (3.46)$$

$$A_2 = (1-\alpha) \left[\exp(T/K_2) - 1\right] \exp(-T/K_2) z^{-1} \left[1 - \exp(-T/K_1)\, z^{-1}\right] \qquad (3.46')$$

Computing the roots of the z-transform of the unit-hydrograph requires setting the numerator $\Lambda(z^{-1})$ to zero and solving the resulting equations. The computation is done numerically using the method described by Kenkins and Traub (1972).

The case of T=1, K_1=5, K_2=20 is considered. The influence of the number of time-steps N and of the value of the parameter α is assessed. For various values of α from 0 to 1, the results for various values of N are shown in Table 3.1. It shows that the value of $|z^{-1}|$ is larger for small values of N and it decreases as N increases. Figure 3.5 presents the Argand diagrams for the cases $N = 40$ and $\alpha = 0$ and $\alpha = 0.25$. Figure 3.6 shows the Argand diagrams for $N = 20$ and $N = 40$ and $\alpha = 0.5$. The latter shows that increasing N adds more points to the same circle essentially.

The problem addressed here is to estimate the values of the model parameters (K_1, K_2, α) from a series of solutions of the above type. This could be attempted using a general purpose optimisation algorithm to estimate the values of the parameters simultaneously. However, in such cases, it very often occurs that a large number of combinations of parameter values give similar model outputs. This is a problem when using automatic parameter estimation procedures. The method described here concentrates on identifying a physically realistic value for each of the parameters in turn. It is easier to estimate the value of the slow reservoir parameter K_2 than the fast one K_1 because the slow component dominates a greater length of the total runoff hydrograph than the fast one. Thus, the first step in the procedure is to estimate the slow component parameter K_2. It can then be separated form the total hydrograph and the parameter of the quick response K_1 may be estimated from the residual hydrograph of shorter duration. Finally, the splitting parameter α is estimated.

N	$\lvert z^{-1}\rvert$				
	α=0 (K_2 only)	α=0.25	α=0.5	α=0.75	α=1.00 (K_1 only)
2	1.051	1.142	1.183	1.206	1.221
4	1.051	1.136	1.178	1.204	1.221
10	1.051	1.118	1.161	1.194	1.221
20	1.051	1.095	1.132	1.170	1.221
40	1.051	1.075	1.096	1.122	1.221
80	1.051	1.063	1.076	1.102	1.221

Table 3.1: Absolute value of the real negative root for two single reservoirs in parallel for different α and timestep N (K_1=5, K_2=20).

3.4.2 Estimation of slow reservoir parameter K_2

An estimate of K_2, noted $\hat{K}_2$, can be calculated by using a high value of N. The numerator mentioned in Equation (3.45) is set to zero:

$$\Lambda\big[H(z^{-1})\big] = 0 \tag{3.47}$$

or:

$$\big[A_1 \exp(-NT/K_1) + A_2 \exp(-NT/K_2)\big]\,(z^{-1})^N = A_1 + A_2 \tag{3.47$'$}$$

For high values of N, since $K_2 > K_1$, $\exp(-NT/K_1)$ becomes negligible compared with $\exp(-NT/K_2)$ and this more than compensates for the fact that $A_1 > A_2$. For values of N of the order of 100 and higher the first term in brackets on the left hand side can be neglected and the equation rewritten as:

$$A_2 \exp(-NT/K_2)\,(z^{-1})^N = A_1 + A_2 \tag{3.48}$$

or in the form:

$$z^{-1} = \left(1 + \frac{A_1}{A_2}\right)^{1/N} \exp(T/K_2) \tag{3.49}$$

If N is sufficient large, z^{-1} converges to $\exp(T/K_2)$ and thus gives an estimate of the parameter K_2.

For the example of $T = 1$, $K_1 = 5$, $K_2 = 20$ and $\alpha = 0.5$, the value of N required may be estimated as follows. The approximation (3.49) becomes:

$$z^{-1} = \left(1 + \frac{0.2214}{0.0554}\right)^{1/N} \exp(T/K_2) \tag{3.50}$$

The average radius of z^{-1} are summarised in Table 3.2. The computer program is used to derive the roots for $N \leq 80$. The above approximation (3.50) is used to derive the roots for $N \geq 80$.

Method	N	$\lvert z^{-1} \rvert$	K_{eq}
Computer	2	1.183	5.9
	4	1.178	6.1
	10	1.161	6.7
	20	1.132	8.1
	40	1.096	10.9
	80	1.076	13.7
Approximation	80	1.072	14.3
	100	1.068	15.1
	200	1.060	17.2
	500	1.055	18.8
	1000	1.053	19.4
	2000	1.052	19.7

Table 3.2: Absolute value of the negative real root and equivalent delay parameter K_{eq} for different time-steps N (K_1=5, K_2=20, α=0.5).

From the above table, it can be concluded that the value of N required to obtain the parameter estimate is of the order of 1000.

For typical cases, the value of N required is in excess of 100 and rounding errors may become significant when computing the polynomial roots using standard precision arithmetic in order to obtain an estimate of the parameter. Since, in practice, with real data, it is not feasible to solve an equation of order 1000, an approximation of the estimate of the slow reservoir parameter $\hat{K_2}$ could be obtained for N=10 and N=100 (denoted $\hat{K}_{N_{10}}$ and $\hat{K}_{N_{100}}$ respectively). Taking $\hat{K}_{N_{1000}} - \hat{K}_{N_{100}} = \hat{K}_{N_{100}} - \hat{K}_{N_{10}}$, it gives the upper bound of $\hat{K_2} = 23.7$. A solution is sought between $\hat{K_2} = 15.1$ and $\hat{K_2} = 23.5$. The average of these estimates is $\hat{K_2} = 19.3$.

3.4.3 Estimation of smaller reservoir K_1

To estimate the parameter of the fast reservoir the beginning of the hydrograph recession is addressed, for which the fast reservoir contribution is essential. For the simplest case, taking the first two ordinates only, i.e. $N = 2$, there are two real roots and the negative

one can be shown to be a close approximation to the root for the fast reservoir in isolation.

For N=2, Equation (3.44) becomes:

$$\begin{aligned} H(z^{-1}) = \alpha \left[\frac{\exp(T/K_1)-1}{T}\right]\exp(-T/K_1)z^{-1}\left[1+\exp(-T/K_1)\,z^{-1}\right] \\ +(1-\alpha)\left[\frac{\exp(T/K_2)-1}{T}\right]\exp(-T/K_2)z^{-1}\left[1+\exp(-T/K_2)\,z^{-1}\right] \end{aligned} \tag{3.51}$$

or:

$$H(z^{-1}) = B_1\left[1+\exp(-T/K_1)\,z^{-1}\right] + B_2\left[1+\exp(-T/K_2)\,z^{-1}\right] \tag{3.52}$$

where:

$$B_1 = \alpha\left[\frac{\exp(T/K_1)-1}{T}\right]\exp(-T/K_1)z^{-1} \tag{3.53}$$

$$B_2 = (1-\alpha)\left[\frac{\exp(T/K_2)-1}{T}\right]\exp(-T/K_2)z^{-1} \tag{3.53$'$}$$

Setting $H(z^{-1})$ to zero and solving for the roots gives:

$$\begin{aligned} z^{-1} &= -\frac{B_1+B_2}{B_1\exp(-T/K_1)+B_2\exp(-T/K_2)} \\ &= -\frac{1+B_2/B_1}{1+B_2/B_1\exp(T/K_1-T/K_2)}\exp(T/K_1) \end{aligned} \tag{3.54}$$

For example, for $T=1$, $K_1=5$, $K_2=20$ and $\alpha=0.5$:

$B_1 = 0.181\,\alpha z^{-1}$,

$B_2 = 0.049\,(1-\alpha)z^{-1}$,

$z^{-1} = 1.186$,

which leads to an equivalent value of K, noted K_{eq}, derived as follows:

$\exp(T/K_{eq}) = 1.186$ whence $K_{eq} = 5.9$.

That is the estimate of K_1, noted $\hat{K}_1$: $\hat{K}_1 = 5.9$.

3.4.4 Estimation of the splitting parameter α

If an estimate of the lag between input and output, noted $U_1^{'}$, is available from a comparison of measured rainfall with discharge data or from some empirical formula, e.g. in terms of the catchment characteristics, then:

$$\alpha\,\hat{K}_1 + (1-\alpha)\,\hat{K}_2 = U_1^{'} \tag{3.55}$$

so that:

$$\alpha = \frac{\hat{K}_2 - U_1^{'}}{\hat{K}_2 - \hat{K}_1} \tag{3.56}$$

In the above example, $U_1^{'} = 0.5(K_1 + K_2) = 12.5$.

Accordingly, the use of the estimates $\hat{K}_1 = 5.9$ and $\hat{K}_2 = 19.5$ would give:

$\alpha = 0.51$, which is close to the value of α=0.50 used in the simulated data.

3.4.5 Refinement of the initial estimates

When preliminary estimates of the rainfall pattern and of the values of K_1 and K_2 have been made, those may be improved by an iterative approach. This is analogous to the application of iteration to the unit-hydrograph by Collins (1939) and to the enhancement of the fast component of the total response by Duband et al. (1993).

When the total response has been divided into the quick response and the slow response, each can be examined to see if the representation can be improved by relaxing the assumption of having a single reservoir (n=1). For a single reservoir (n=1), the root pattern is a single circle and the value of the negative real root is z^{-1}= - exp(T/K). For integer values of $n > 1$, there is a root at the origin. Where such a root occurs, the best assumption based on experience would be to take n=2. For n=3, there will be three roots: 0, +1 and -1/2 so that z^{-1}=$-1/2 \exp(T/K)$.

3.4.6 Enhancement of the slow response

The relative contribution of the quicker component can be enhanced by forward differentiating the outflow hydrograph and then analysing the resulting time-series. However, this tends to enhance any errors in the flow data at the expense of the underlying information. In contrast, auto-correlation, which enhances the slow component, reduces the effect of any data errors by smoothing the total response. This is developed here.

The K_2 component in the catchment response can be amplified and the effect of measurement noise greatly reduced by using the auto-correlation function $\rho(\tau)$ of the output $y(t)$ as the subject of analysis. The auto-correlation function is defined as:

$$\rho(\tau) = \int_0^\infty y(t)\, y(t+\tau)\, dt \tag{3.57}$$

where τ is a time displacement parameter. In the present case, the output is the unit-hydrograph $h(t)$:

$$y(t) = h(t) = \alpha\, a \exp(-a\, t) + (1-\alpha)\, b \exp(-b\, t) \tag{3.58}$$

where $a = T/K_1$ and $b = T/K_2$. Then:

$$\rho(\tau) = \left[\frac{\alpha^2}{2} + \frac{\alpha(1-\alpha)b}{a+b}\right] a \exp(-a\tau) + \left[\frac{(1-\alpha)^2}{2} + \frac{\alpha(1-\alpha)a}{a+b}\right] b \exp(-b\tau) \tag{3.59}$$

For the example of $\alpha = 0.5$, $a = T/K_1 = 0.2$ and $b = T/K_2 = 0.05$, this gives:

$$\rho(\tau) = \frac{1}{4}\left(\frac{1}{2} + \frac{b}{a+b}\right) a \exp(-a\tau) + \frac{1}{4}\left(\frac{1}{2} + \frac{a}{a+b}\right) b \exp(-b\tau) \tag{3.60}$$

which, compared with Equation (3.58), increases the weighting of $b\exp(-b\tau)$ from 50% to 65%, or almost a ratio of 2:1. A further auto-correlation would produce a weighting of 82% which would further increase the estimate of K_2.

3.5 Conclusion and discussion

The aim of this study has been to develop a reliable method of unit-hydrograph derivation for flood forecasting from events for which the estimates of effective rainfall are unreliable or non-existent. Such a method depends on the extraction of an estimated unit-hydrograph solely from the data for catchment runoff.

For the case of sampling interval T=1 and a linear reservoir with a lag time of K, analysis indicates a z-transform root pattern on the Argand diagram of a perfect circle with a radius of $\exp(T/K)$. Numerical experiments reproduced the expected values for all lengths of records from N=2 to N=80 as shown in Table 3.1. This was considered sufficient to validate the stability and accuracy of the computer program used.

For the case of two linear reservoirs (K_1 and K_2) in parallel with a proportion α of the total flow through the fast response reservoir K_1, numerical experiments were conducted for various parameters values. For the values of α other than 0 and 1, the root pattern no longer forms a perfect circle. The new method was validated on synthetic data corresponding to $\alpha = 0.5, K_1 = 5, K_2 = 20$. The fast reservoir parameter K_1 was obtained using the first two ordinates of the recession whereas the slow reservoir parameter K_2 was derived using the long series of ordinates, up to 1000.

For real cases, with measured river discharge data, it is advised to use the first few ordinates (fewer than ten) of the recession part of the hydrograph to estimate the fast

reservoir parameter. Depending on which part of the slow recession needs to be modeled, the length of the series of ordinates may vary. It is advised to start with the ordinate corresponding to the beginning of the baseflow contribution. The splitting parameter α may then best estimated using a priori knowledge on the lag between the rainfall input and the catchment response.

In the case of parallel response functions, the slower response signal can be enhanced by taking the autocorrelation function of the output data. For the synthetic example shown with α=0.5, a single use of autocorrelation increases the representation of flow through the slower response from 50% to 65%. A second autocorrelation would increase the proportion further from 65% to 82%. The use of autocorrelation on real data should smooth out the effect of data errors.

The work described above represents a new step in the development of the root matching-root selection approach, due to De Laine and Turner respectively. It is proposed to distinguish it from the previous versions of this general approach by describing it as the "root separation method".

The four disadvantages of the original root-matching method of de Laine (1970) as described by Turner et al. (1989) were quoted in the chapter. The first two disadvantages are overcome by the root selection method (Turner, 1982; Turner et al., 1989) since the shift in the actual values of the polynomial does not affect the overall pattern. A difficulty remains in the case of uniform effective rainfall or an extremely U-shaped distribution of rainfall, both of which give rise to a circular pattern of rainfall roots which may not be readily separated from the response roots for a single reservoir. The third disadvantage, related to the effects of choice of method of baseflow separation, is overcome by separating the root pattern of the total response into its component parts. In the example given, the reduction of total rainfall to effective rainfall is on the basis of a single coefficient. This can be extended to other forms of separation, but this question is not addressed here. In regard to the fourth disadvantage, the assumption of linearity, there is a possibility of extending the approach to the case of non-linearity (Dooge, 1967) but this is also outside the scope of the present study.

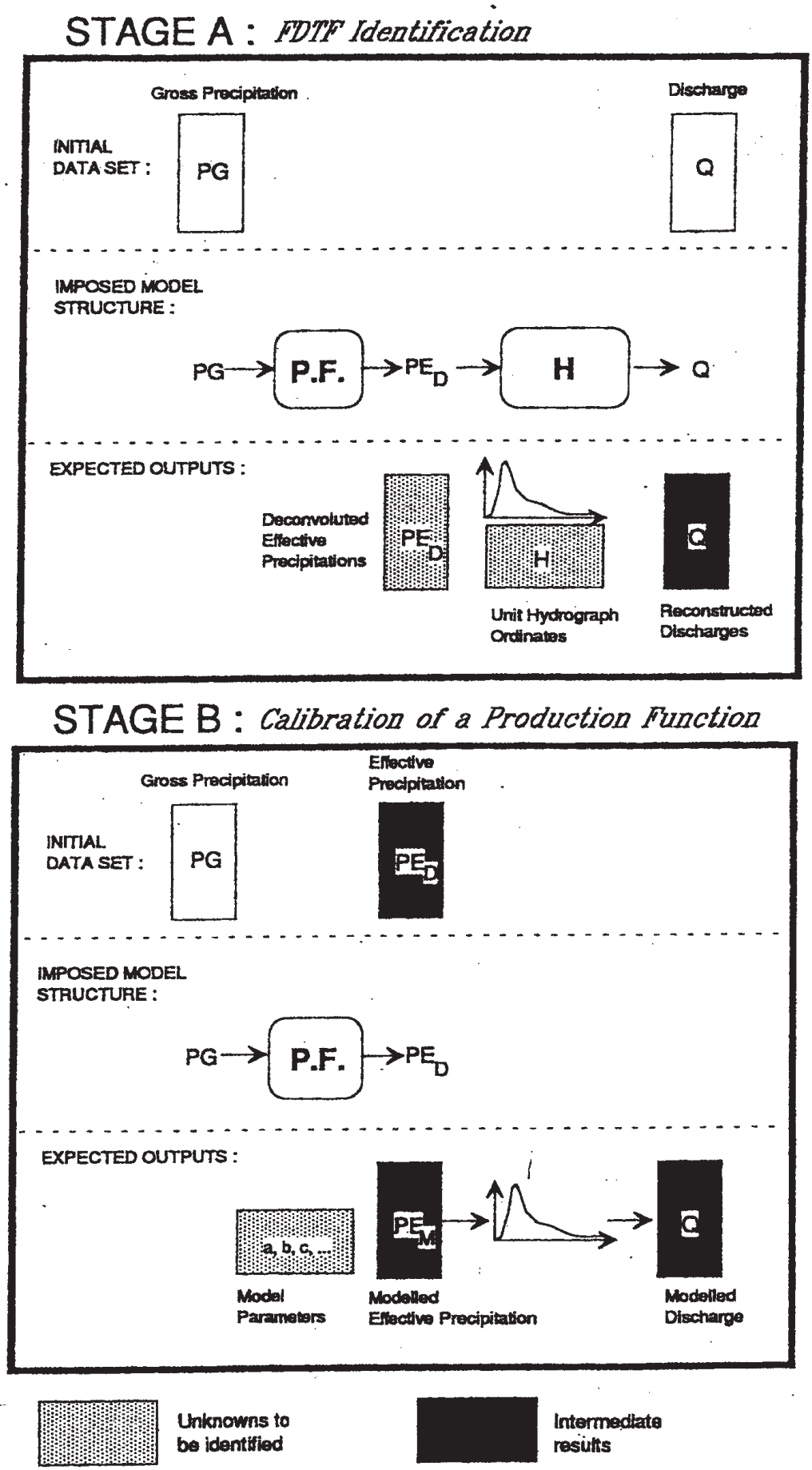

Figure 3.1: FDTF method summary

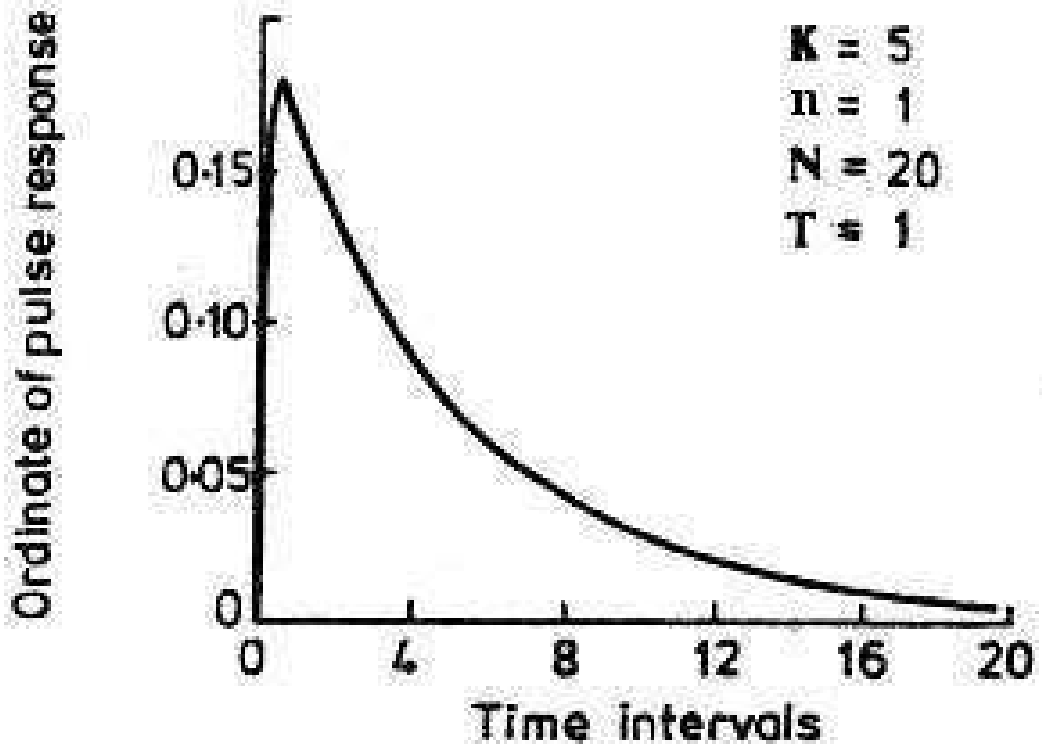
K = 5
n = 1
N = 20
T = 1
Ordinate of pulse response
0·15
0·10
0·05
0
0
4
8
12
16
20
Time intervals

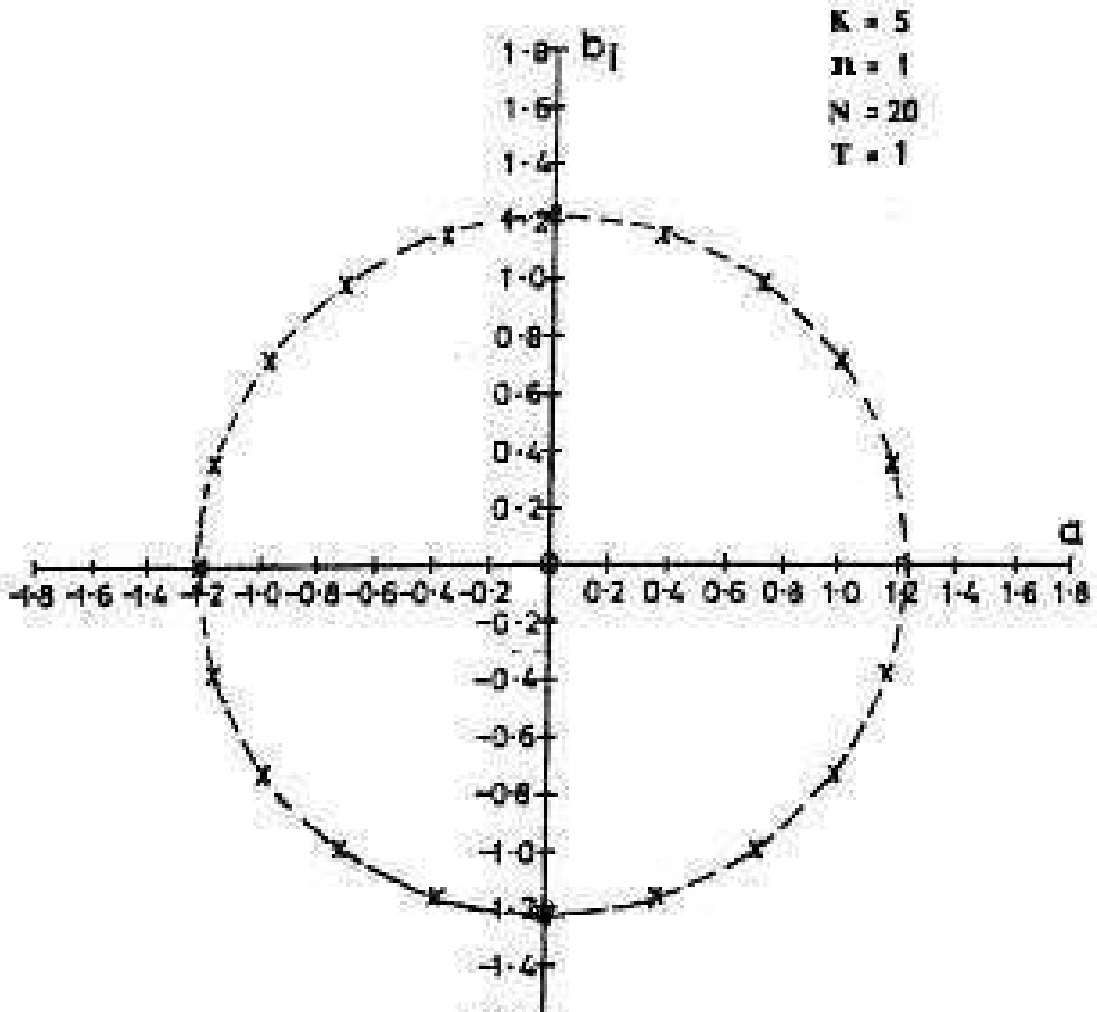
K = 5
n = 1
N = 20
T = 1
b1
a
1·8
1·6
1·4
1·2
1·0
0·8
0·6
0·4
0·2
-0·2
-0·4
-0·6
-0·8
-1·0
-1·2
-1·4
-1·8 -1·6 -1·4 -1·2 -1·0 -0·8 -0·6 -0·4 -0·2
0·2 0·4 0·6 0·8 1·0 1·2 1·4 1·6 1·8

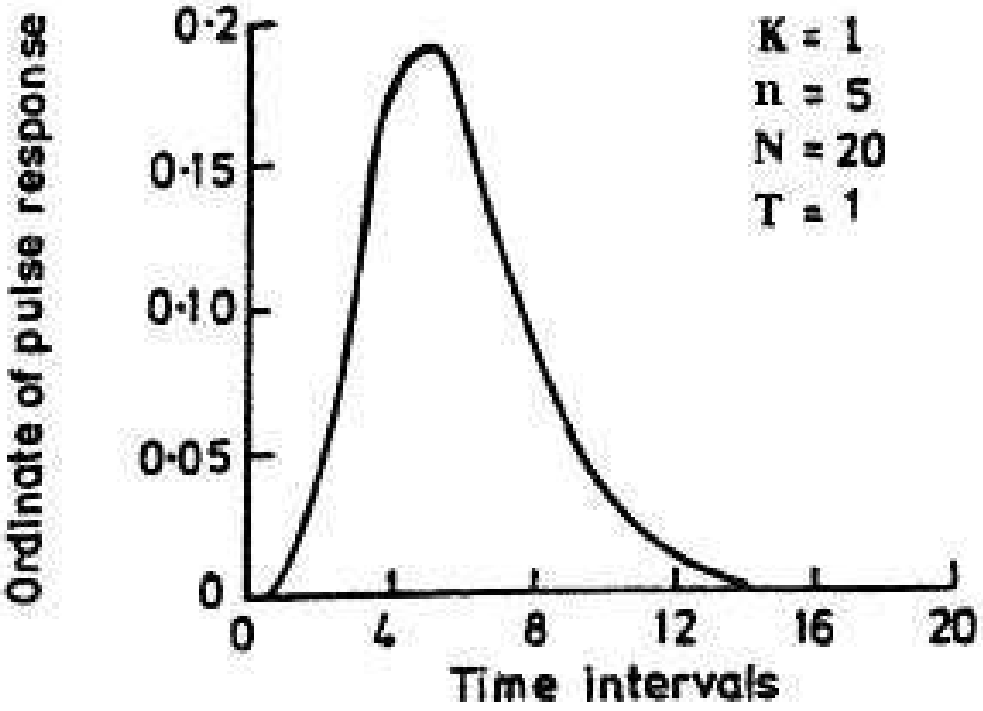
Ordinate of pulse response
0·2
0·15
0·10
0·05
0
0
4
8
12
16
20
Time intervals
K = 1
n = 5
N = 20
T = 1

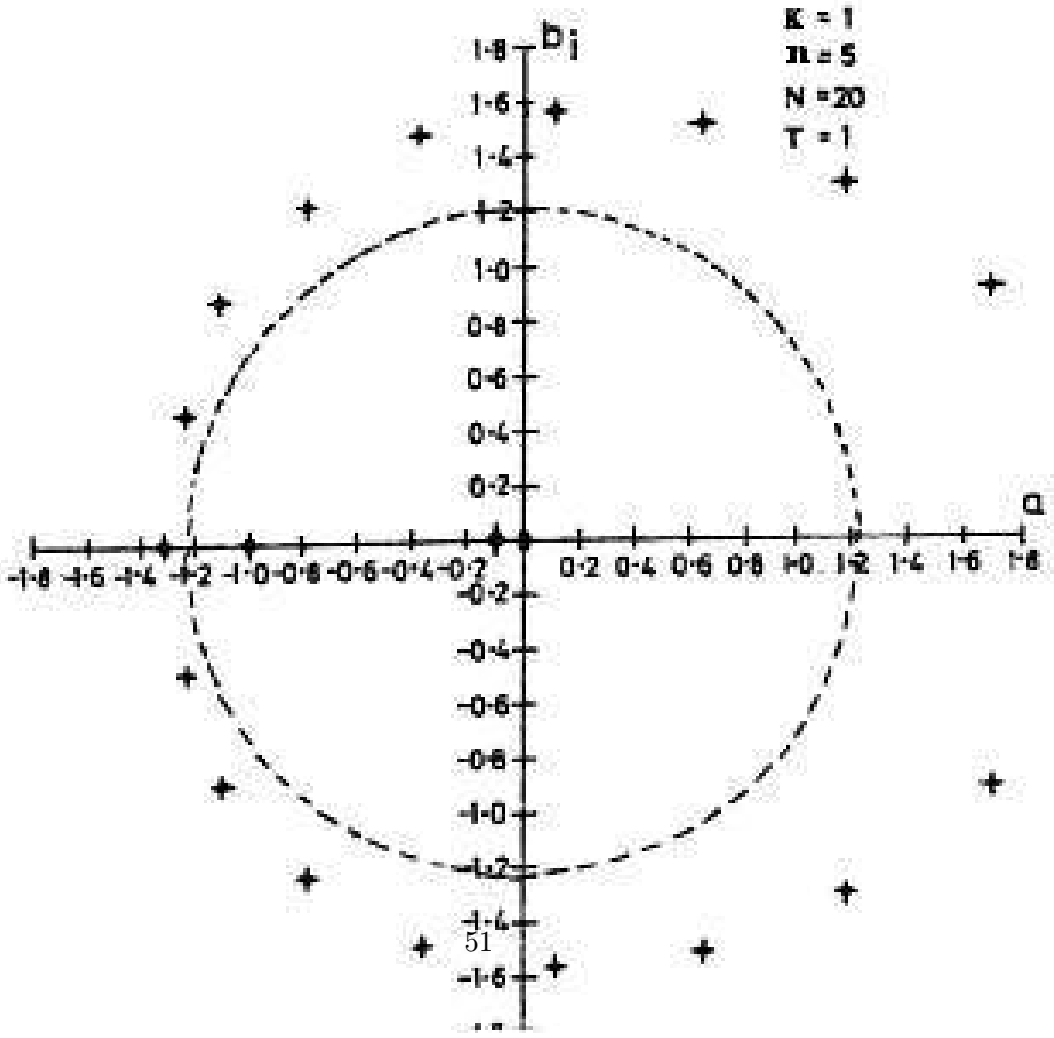
bi
a
K = 1
n = 5
N = 20
T = 1

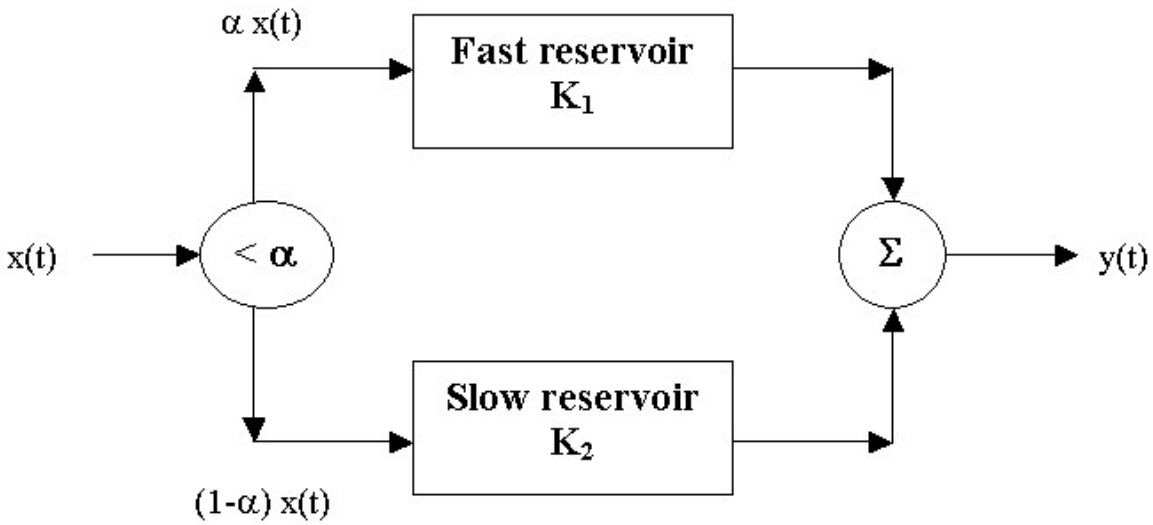

Figure 3.4: 2 linear reservoirs model

2 single reservoirs in parallel, alpha=0, N=40

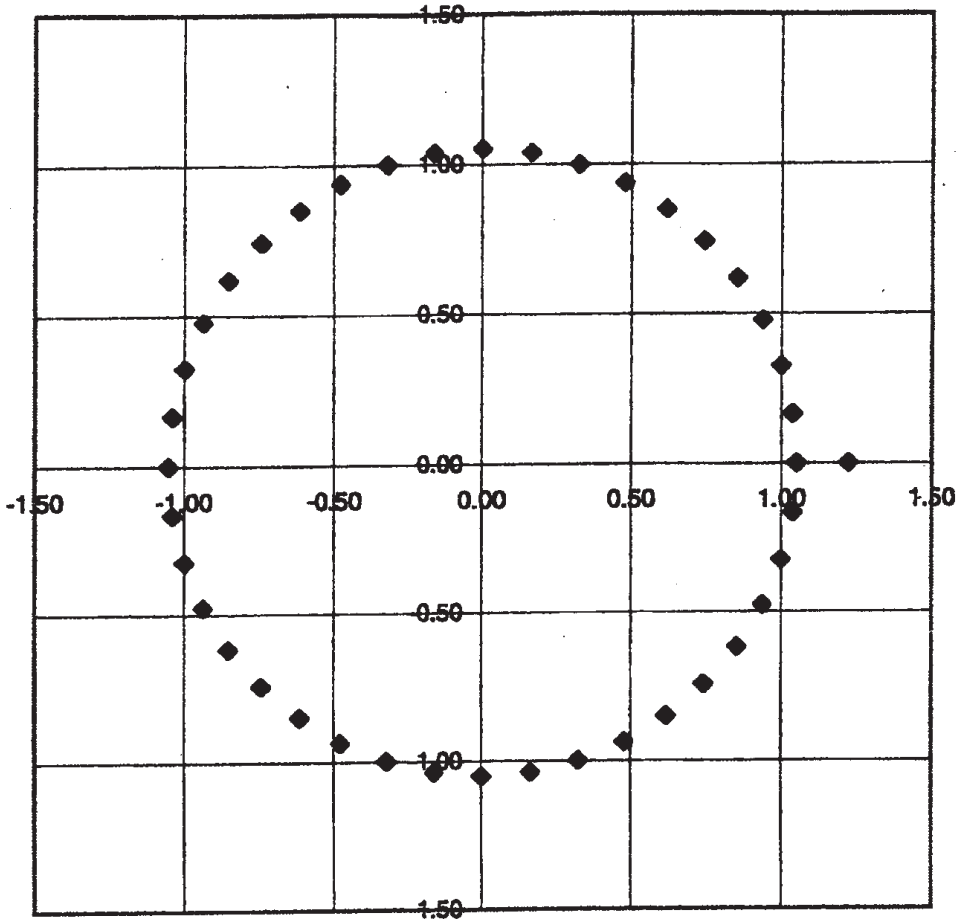

2 single reservoirs in parallel, alpha=0.25, N=40

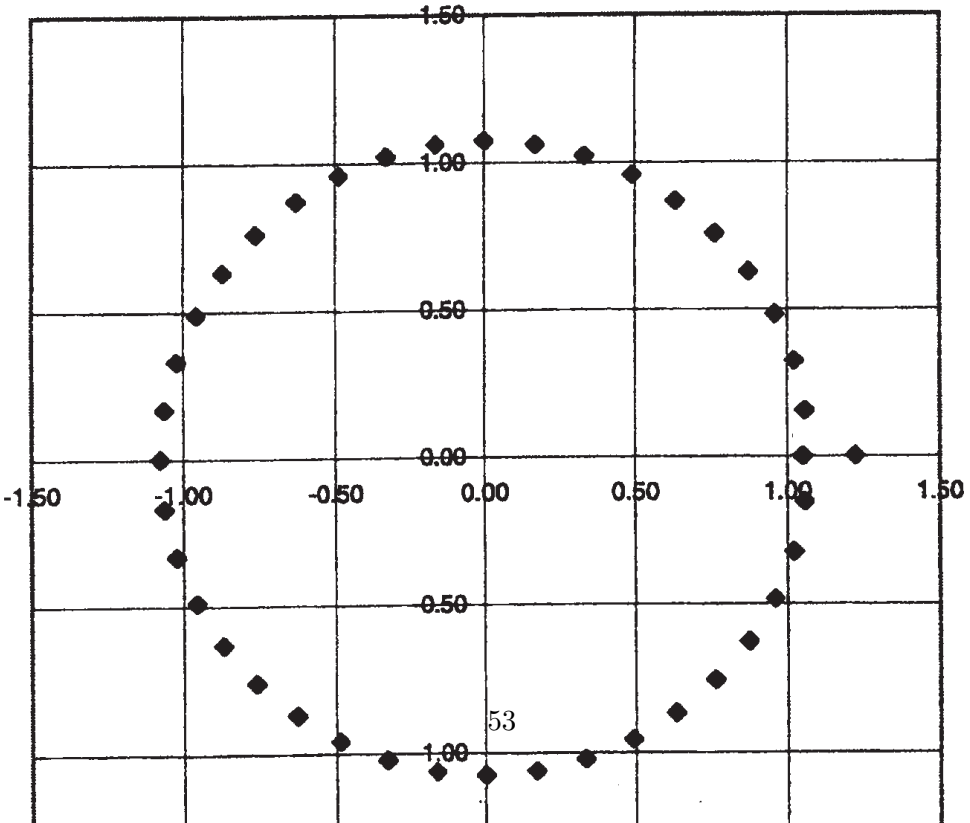

2 single reservoirs in parallel, alpha=0.5, N=20

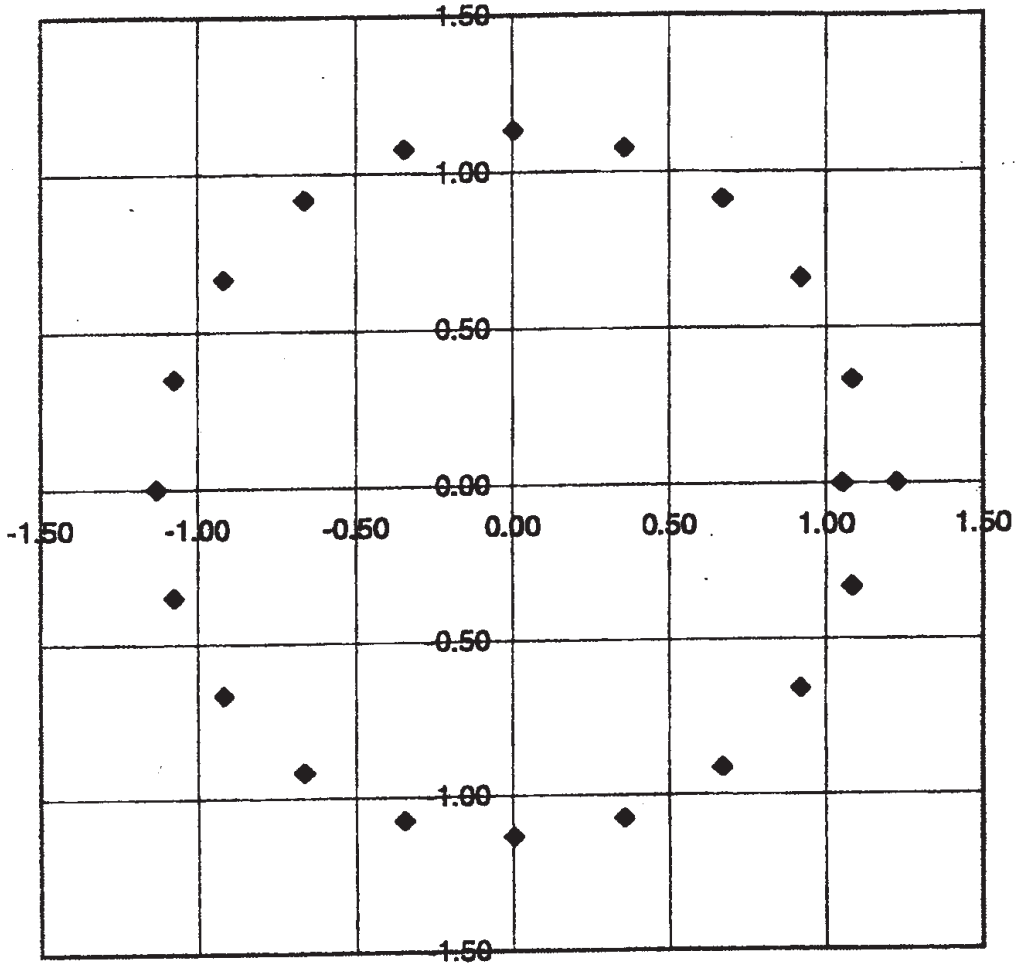

2 single reservoirs in parallel, alpha=0.5, N=40

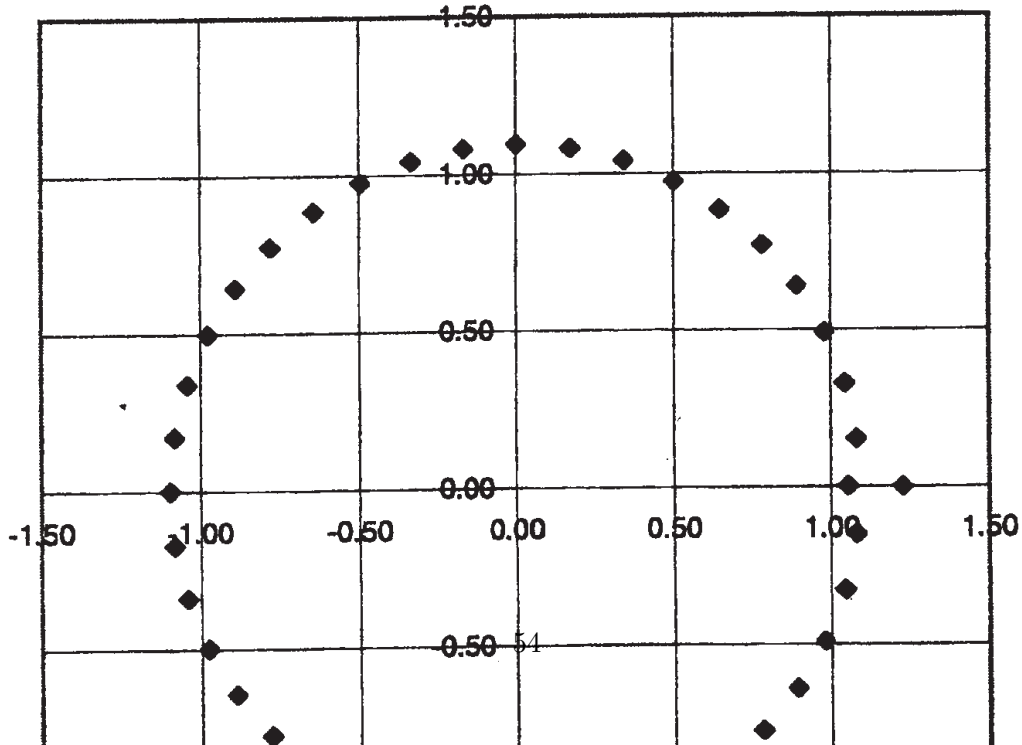

Bibliography

Box, G. E. P. and Jenkins, G. M. (1976). *Time Series Analysis. Forecasting and Control*. Holden Day, San Franciso, U.S. 3^{rd} edition by G.E.P. Box, G.M. Jenkins and G.C. Reissel, Prentice Hall, New Jersey, 1994.

Bruen, M. and Dooge, J. C. I. (1984). An efficient and robust method for estimating unit-hydrograph ordinates. *Journal of Hydrology*, 70:1–24.

Collins, W. T. (1939). Runoff distribution graphs for precipitation occurring in more than one time unit. *Civil Eng.*, 9(9):559–561.

de Laine, R. J. (1970). Deriving the unit-hydrograph without using rainfall data. *Journal of Hydrology*, 10:379–390.

de Laine, R. J. (1975). *Identifying a time-invariant system from its inputs*. PhD thesis, Monach University, Victoria, Australia.

Dooge, J. C. I. (1967). A new approach to non-linear problems in surface water hydrology. In *Proc. IAHS General Assembly, Bern*, pages 409–413.

Dooge, J. C. I. (1979). Deterministic input-output models. In E. H. Lloyd, T. O. and Wilkinson, J. C., editors, *The Mathematics of Hydrology and Water Resources*. Academic Press, London, UK.

Duband, C., Obled, C., and Rodriguez, J. Y. (1993). Unit-hydrograph revisited: an alternative iterative approach to unit-hydrograph and effective rainfall identification. *Journal of Hydrology*, 150:115–149.

Gouy, D. (1991). Comparaison de deux méthodes d'identification de la fonction de transfert et des pluies efficaces: application au bassin du gardon d'anduze. Mémoire de DEA, Un. Joseph Fourier, INPG, Grenoble, France.

Guillot, P. and Duband, D. (1980). Une méthode de transfert pluie-debit par régression multiple. In *Proc. Oxford Symp. Hydrological Forecasting*, pages 129:177–186. IAHS Publ.

Hoerl, A. E. and Kennard, R. W. (1970). Ridge regression, biaised estimation for non-orthogonal problems. *Technometrics*, 12(1):55–67.

Jakeman, A. J., Littlewood, I. G., and Whitehead, P. G. (1990). Computation of the instantaneous unit-hydrograph and identifiable component flows with application to two small upland catchments. *Journal of Hydrology*, 117:275–300.

Kenkins, M. A. and Traub, J. F. (1972). Zeros of a complex polynomial, algorithm no.419. *Comm. Assoc. Computing Machinery*, 15:97.

Nalbantis, I. (1987). *Identification de modèles pluie-débit du type hydrogramme unitaire: développement de la méthode DPFT et validation sur données générées.* PhD thesis, INPG, Grenoble, France.

Nalbantis, I., Obled, C., and Rodriguez, J. Y. (1995). Unit-hydrograph and effective rainfall identification. *Journal of Hydrology*, 168:127–157.

Nash, J. E. (1958). The form of the instantaneous hydrograph. In *Gen. Ass. Toronto*, pages 3:114–118. IAHS Publ. No. 42.

Natale, L. and Todini, E. (1976). A stable estimator for linear models 1-theoretical development and monte-carlo experiments. *Water Resources Research*, 12(4):667–671.

Newton, D. W. and Vineyard, J. W. (1967). Computer determined unit-hydrograh from flows. *Journal of Hydraulics DIV. ASCE. 93*, HY5:219–235.

Obled, C. (1989). Reflections on rainfall information requirements for operational rainfall-runoff modeling. In *Proc. Int. Symp. Hydrol. App. Weather Radar*, pages 469–482. Un. Salford, UK.

O'Connor, K. M. (1976). A discrete linear cascade for hydrology. *Journal of Hydrology*, 29:203–242.

O'Connor, K. M. (1982). Derivation of discretely coincident forms of continuous time-invariant models using the transfer function approach. *Journal of Hydrology*, 59:1–48.

Saucedo, R. and Schiring, E. E. (1968). *Introduction to Continuous and Digital Control Systems.* MacMillan, New-York, USA.

Turner, J. E. (1982). A real-time flood forecasting model for the river liffey. Master's thesis, University College Dublin, Ireland.

Turner, J. E., Dooge, J. C. I., and Bree, T. (1989). Deriving the unit-hydrograph by root selection. *Journal of Hydrology*, 110:137–152.

Versiani, B. (1983). *Modélisation pluie-débit pour la prévision des crues.* PhD thesis, USMG/INPG, Grenoble, France.

Wilson, J. W. (1970). Integration of radar and raingauge data for improved rainfall measurement. *Journal of Applied Meteorology*, 9:489–497.

Wood, S. J., Jones, D. A., and Moore, R. J. (2000). Static and dynamic calibration of radar data for hydrological use. *Hydrology and Earth System Sciences*, (4):545–554.

Wormleaton, M. (1980). Discussion on optimization of unit-hydrograph determination. *Journal of Hydraulics Dic. ASCE*, 106(HY12):2076–2078.